The two-photon exchange contribution to elastic electron-nucleon scattering at large momentum transfer

Andrei V. Afanasev,[1, *] Stanley J. Brodsky,[2, †] Carl E. Carlson,[3, ‡]

Yu-Chun Chen,[4, §] and Marc Vanderhaeghen[1, 3, ¶]

[1]*Thomas Jefferson National Accelerator Facility, Newport News, VA 23606, USA*

[2]*SLAC, Stanford University, Stanford, CA 94309, USA*

[3]*Department of Physics, College of William and Mary, Williamsburg, VA 23187, USA*[‡]

[4]*Department of Physics, National Taiwan University, Taipei 10617, Taiwan*

(Dated: January 31, 2005)

Abstract

We estimate the two-photon exchange contribution to elastic electron-proton scattering at large momentum transfer by using a quark-parton representation of virtual Compton scattering. We thus can relate the two-photon exchange amplitude to the generalized parton distributions which also enter in other wide angle scattering processes. We find that the interference of one- and two-photon exchange contribution is able to substantially resolve the difference between electric form factor measurements from Rosenbluth and polarization transfer experiments. Two-photon exchange has additional consequences which could be experimentally observed, including nonzero polarization effects and a positron-proton/electron-proton scattering asymmetry. The predicted Rosenbluth plot is no longer precisely linear; it acquires a measurable curvature, particularly at large laboratory angle.

PACS numbers: 25.30.Bf, 13.40.Gp, 24.85.+p

[*]afanas@jlab.org

[†]sjbth@slac.stanford.edu

[‡]carlson@physics.wm.edu

[§]snyang1@phys.ntu.edu.tw

[¶]marcvdh@jlab.org

I. INTRODUCTION

There are two experimental methods for extracting the ratio of electric (G_E^p) to magnetic (G_M^p) proton form factors from electron-proton scattering: unpolarized measurements employing the Rosenbluth separation technique, and polarization experiments. In the latter case, one measures the correlation of the spin of the incident polarized electron with the polarization components of the outgoing proton, parallel P_l or perpendicular P_s (in the scattering plane) to its momentum [1, 2, 3]. The ratio of cross sections for the two outgoing proton polarizations gives G_E/G_M directly:

$$\frac{P_s}{P_l} = -\sqrt{\frac{2\varepsilon}{\tau(1+\varepsilon)}} \frac{G_E(Q^2)}{G_M(Q^2)} \ . \tag{1}$$

The kinematic functions ε and τ are

$$\tau \equiv \frac{Q^2}{4M^2} \ , \tag{2}$$

and

$$\frac{1}{\varepsilon} \equiv 1 + 2(1+\tau)\tan^2\frac{\theta}{2} \ , \tag{3}$$

where $Q^2 = -q^2 = -t$ is the momentum transfer squared, θ is the laboratory scattering angle, and $0 \leq \varepsilon \leq 1$. Equivalent information may be obtained in scattering of longitudinally polarized electrons on a polarized proton target.

The Rosenbluth method relies on measuring the differential cross section

$$\frac{d\sigma}{d\Omega_{Lab}} \propto G_M^2 + \frac{\varepsilon}{\tau}G_E^2 \ , \tag{4}$$

with the proportionality factor being well known, and isolating the ε dependent term. In each case, the extraction method for G_E/G_M assumes single-photon exchange between the electron and nucleon.

Recent polarization experiments at the Thomas Jefferson Laboratory (JLab) [4, 5] have confirmed the earlier Rosenbluth measurements from SLAC [6]. However, at large Q^2, all of the Rosenbluth measurements are at distinct variance with JLab measurements of G_E^p/G_M^p obtained using the polarization technique [1, 2]. Since G_E^p contributes to the unpolarized cross section at only a few percent level for the Q^2 range in question, it is necessary to

identify any possible systematic corrections to the Rosenbluth measurements at the percent level which could be responsible for this discrepancy.

One possible explanation for the discrepancy between the Rosenbluth and polarization methods is the presence of two-photon exchange effects, beyond those which have already been accounted for in the standard treatment of radiative corrections. A general study of two- (and multi)-photon exchange contributions to the elastic electron-proton scattering observables was given in [7]. In that work, it was noted that the interference of the two-photon exchange amplitude with the one-photon exchange amplitude could be comparable in size to the $(G_E^p)^2$ term in the unpolarized cross section at large Q^2. In contrast, the two-photon exchange effects do not impact the polarization-transfer extraction of G_E/G_M in an equally significant way. Thus a missing and unfactorizable part of the two-photon exchange amplitude at the level of a few percent may well explain the discrepancy between the two methods.

Realistic calculations of elastic electron-nucleon scattering beyond the Born approximation are required in order to demonstrate in a quantitative way that two-photon exchange effects are indeed able to resolve this discrepancy. In particular, one wants to study quantitatively the "hard" corrections which will arise when both exchanged photons are far off shell or the intermediate nucleon state suffers inelastic excitations. Calculations of these corrections require a knowledge of the internal structure of the nucleon and thus could not be included in the classic [8, 9] and were not included in the more recent [10, 11] calculations of radiative corrections to eN elastic scattering.

A first step was performed recently in [12], where the contribution to the two-photon exchange amplitude was calculated for the elastic nucleon intermediate state. In that calculation it was found that the two-photon exchange correction with an intermediate nucleon has the proper sign and magnitude to partially resolve the discrepancy between the two experimental techniques.

In an earlier short note [13], we reported the first calculation of the hard two-photon elastic electron-nucleon scattering amplitude at large momentum transfers by relating the required virtual Compton process on the nucleon to generalized parton distributions (GPD's) which also enter in other wide angle scattering processes. This approach effectively sums all possible excitations of inelastic nucleon intermediate states. We found that the two-photon corrections to the Rosenbluth process indeed can substantially reconcile the two ways of

measuring G_E/G_M. Our goal in this paper is to give a detailed account of our work, and to present numerical results for a number of quantities not included in the shorter report.

Perturbative QCD factorization methods for hard exclusive processes provide a systematic method for computing the scaling and angular dependence of real and virtual Compton scattering at large t. For example, PQCD predicts that the leading-twist amplitude for Compton scattering $\gamma p \rightarrow \gamma p$ can be factorized as a product of hard-scattering amplitudes $T_H(\gamma qqq \rightarrow \gamma qqq)$, where the quarks in each proton are collinear, convoluted with the initial and final proton distribution amplitudes $\phi(x_i, Q)$ [14]. All of the hard-scattering diagrams fall at the same rate at large momentum transfer whether or not the photons interact on the same line. Although, the predictions for the power-law falloff and angular dependence of Compton scattering are consistent with experiment, the leading-twist PQCD calculations of the wide angle Compton amplitudes appear to substantially underpredict the magnitude of the observed Compton cross sections [15].

Since an exact QCD analysis of virtual Compton scattering does not appear practical, we have modeled the hard two-photon exchange amplitude using the "handbag approximation" [16], in which both photons interact with the same quark. The struck quark is treated as quasi-on shell. In particular, we have neglected the amplitudes where the two hard protons connect to different quarks, the "cat's ears" diagrams, as well as the diagrams in which gluons interact on the fermion line between the two currents. The handbag diagrams contain the "$J = 0$" fixed pole, the essential energy-independent contribution to the real part of Compton amplitude which arises due to the local structure of the quark current [17, 18]. The handbag approximation has proven phenomenologically successful in describing wide-angle Compton scattering at moderate energies and momentum transfers. As we shall show, the handbag approximation allows the two-photon exchange amplitude to be linked to the generalized parton distributions (GPD's) [19, 20, 21], thus providing considerable phenomenological guidance.

Brooks and Dixon and Vanderhaeghen *et al.* [15] have shown that PQCD diagrams where the photons attach to the same quark dominate the Compton amplitude on the proton, except at backward center-of-mass angles.[1]. The dominance of the handbag diagrams in the

---

[1] This suppression of the cat's ears diagrams at forward angles could be due to the momentum mismatches which occur when photons couple to different quarks. Another possible explanation is that in some kinematic regions, the cat's ears and handbag amplitudes have the same magnitude (or nearly so) except

PQCD analysis provides some justification for the the use of the handbag approximation. However, it should be noted that Gunion and Blankenbecler [22] have shown that electron-deuteron scattering is dominated by the cat's ears diagrams at large momentum transfer provided that the deuteron wave function has Gaussian fall-off. The dominance of the handbag diagrams thus depends on the nature of the QCD wave functions, and the precise situation in the present case remains a subject for future study.

Recently, a new category of Rosenbluth data has become available where the recoiling proton is detected [23]. The new data appear to confirm the older data, where the scattered electron was detected. The two-photon exchange contributions are the same whatever particle is detected. However, the bremsstrahlung corrections, which are added to obtain an infrared finite result, are different. We shall defer detailed discussion of the proton-detected data until we can reevaluate the original proton-observed electron-proton bremsstrahlung interference calculations [9, 24] as well as examine the radiative corrections which have been applied to the new data [23, 25].

The plan of this paper is as follows:

The next section is devoted to kinematics, including the definitions of the invariants which define the scattering amplitudes and the formulae for the cross sections and polarizations in terms of those invariants. There are choices in the definitions of the invariants. We have presented the bulk of the paper with one choice; a sometimes useful alternative choice is summarized with cross section and polarization formulas in Appendix A. Section III gives analytic results for the two-photon exchange scattering amplitudes at the electron-quark level, the hard scattering amplitudes required for the partonic calculation of two-photon exchange in electron-nucleon scattering. We have generally treated the quarks as massless. A quantitative discussion of modifications following from finite quark mass appears in Appendix B. Section IV details the embedding of the partonic amplitude within the nucleon scattering amplitude, using dominance of handbag amplitudes and GPD's. This section also

---

for the charge factors. In these regions, the Compton amplitude would be proportional to the total charge squared $(2e_u + e_d)^2$ of the target proton. This is precisely the case in the low energy limit, where the Compton amplitude is indeed proportional to $(2e_u + e_d)^2 = 1$ for a proton. The result is reproduced by the handbag diagrams alone since, coincidentally, $2e_u^2 + e_d^2 = 1$. In this scenario, the handbag approximation will fail for Compton scattering on a neutron or deuteron target. At higher energies, discussion of this scenario pertains to large angle Compton scattering, since in the forward direction the handbag diagrams are known to dominate.

discusses the particular GPD's which we have used in our numerical calculations. Section V shows numerical results, given graphically, for cross sections, single spin asymmetries, polarization transfers, and positron-proton vs. electron-proton comparisons. Section V also includes commentary about the possibility of extending the calculations to backward scattering (small values of $|u|$), and an assessment of how well two-photon physics reconciles the Rosenbluth and polarization transfer measurements of G_E/G_M. Section VI summarizes our conclusions.

II. ELASTIC ELECTRON-NUCLEON SCATTERING OBSERVABLES

In order to describe elastic electron-nucleon scattering,

$$l(k, h) + N(p, \lambda_N) \rightarrow l(k', h') + N(p', \lambda'_N), \tag{5}$$

where h, h', λ_N, and λ'_N are helicities, we adopt the definitions

$$P = \frac{p + p'}{2}, \ K = \frac{k + k'}{2}, \ q = k - k' = p' - p \ , \tag{6}$$

define the Mandelstam variables

$$s = (p + k)^2, \quad t = q^2 = -Q^2, \quad u = (p - k')^2, \tag{7}$$

let $\nu \equiv K \cdot P$, and let M be the nucleon mass.

The T-matrix helicity amplitudes are given by

$$T^{h',h}_{\lambda'_N, \lambda_N} \equiv \langle k', h'; p', \lambda'_N | T | k, h; p, \lambda_N \rangle \ . \tag{8}$$

Parity invariance reduces the number of independent helicity amplitudes from 16 to 8. Time reversal invariance further reduces the number to 6 [26]. Further still, in a gauge theory lepton helicity is conserved to all orders in perturbation theory when the lepton mass is zero. We shall neglect the lepton mass. This finally reduces the number of independent helicity amplitudes to 3, which one may for example choose as

$$T^{+,+}_{+,+} \ ; \quad T^{+,+}_{-,-} \ ; \quad T^{+,+}_{-,+} = T^{+,+}_{+,-} \ . \tag{9}$$

(The phase in the last equality is for particle momenta in the xz plane, and is valid whether we are in the center-of-mass frame, the Breit frame, or the symmetric frame to be defined below.)

6

Alternatively, one can expand in terms of a set of three independent Lorentz structures, multiplied by three generalized form factors. Only vector or axial vector lepton currents can appear in order to ensure lepton helicity conservation. A possible T-matrix expansion is (removing an overall energy-momentum conserving δ-function),

$$T_{h,\lambda_N'\lambda_N} = \frac{e^2}{Q^2} \left\{ \bar{u}(k',h)\gamma_\mu u(k,h) \times \bar{u}(p',\lambda_N') \left[\gamma^\mu G_M' - \frac{P^\mu}{M}F_2'\right] u(p,\lambda_N) \right.$$
$$\left. + \bar{u}(k',h)\gamma_\mu\gamma_5 u(k,h) \times \bar{u}(p,\lambda_N') \gamma^\mu\gamma^5 G_A' u(p,\lambda_N) \right\} . \tag{10}$$

This expansion is general. The overall factors and the notations G_M' and F_2' have been chosen to have a straightforward connection to the standard form factors in the one-photon exchange limit.

There is no lowest order axial vector vertex in QED: the effective axial vertex in the expansion arises from multiple photon exchanges and vanishes in the one-photon exchange limit. One may eliminate the axial-like term using the identity

$$\bar{u}(k')\gamma \cdot P u(k) \times \bar{u}(p')\gamma \cdot K u(p) = \frac{s-u}{4} \bar{u}(k')\gamma_\mu u(k) \times \bar{u}(p')\gamma^\mu u(p)$$
$$+ \frac{t}{4} \bar{u}(k')\gamma_\mu\gamma_5 u(k) \times \bar{u}(p')\gamma^\mu\gamma^5 u(p) , \tag{11}$$

which is valid for massless leptons and any nucleon mass. Hence, an equivalent T-matrix expansion is

$$T_{h,\lambda_N'\lambda_N} = \frac{e^2}{Q^2} \bar{u}(k',h)\gamma_\mu u(k,h) \tag{12}$$
$$\times \bar{u}(p',\lambda_N') \left(\tilde{G}_M \gamma^\mu - \tilde{F}_2\frac{P^\mu}{M} + \tilde{F}_3\frac{\gamma \cdot K P^\mu}{M^2} \right) u(p,\lambda_N) .$$

Knowing both expansions of the scattering amplitude is useful, particularly when making comparison to other work. Our analysis will primarily use the second expansion, with the invariants denoted with tildes. A selection of expressions using the primed invariants is given in Appendix A.

The scalar quantities $\tilde{G}_M$, $\tilde{F}_2$, and $\tilde{F}_3$ are complex functions of two variables, say ν and Q^2. We will also use

$$\tilde{G}_E \equiv \tilde{G}_M - (1+\tau)\tilde{F}_2 . \tag{13}$$

In order to easily identify the one- and two-photon exchange contributions, we introduce the notation $\tilde{G}_M = G_M + \delta\tilde{G}_M$, and $\tilde{G}_E = G_E + \delta\tilde{G}_E$, where G_M and G_E are the usual

proton magnetic and electric form factors, which are functions of Q^2 only and are defined from matrix elements of the electromagnetic current. The amplitudes $\tilde{F}_3 = \delta\tilde{F}_3$, $\delta\tilde{G}_M$, and $\delta\tilde{G}_E$, originate from processes involving the exchange of at least two photons, and are of order e^2 (relative to the factor e^2 in Eq. (12)).

The cross section without polarization is

$$\frac{d\sigma}{d\Omega_{Lab}} = \frac{\tau\sigma_R}{\epsilon(1+\tau)}\frac{d\sigma_{NS}}{d\Omega_{Lab}} , \tag{14}$$

where $\tau \equiv Q^2/(4M^2)$, ε is

$$\varepsilon = \left(1 + 2(1+\tau)\tan^2\frac{\theta}{2}\right)^{-1} = \frac{(s-u)^2 + t(4M^2 - t)}{(s-u)^2 - t(4M^2 - t)} , \tag{15}$$

θ is the electron Lab scattering angle, the "no structure" cross section is

$$\frac{d\sigma_{NS}}{d\Omega_{Lab}} = \frac{4\alpha^2\cos^2\frac{\theta}{2}}{Q^4}\frac{E'^3}{E} , \tag{16}$$

and E and E' are the incoming and outgoing electron Lab energies. For one-photon exchange, ε is the polarization parameter of the virtual photon. The reduced cross section including the two-photon exchange correction is given by [7]

$$\sigma_R = G_M^2 + \frac{\varepsilon}{\tau}G_E^2 + 2\,G_M\mathcal{R}\left(\delta\tilde{G}_M + \varepsilon\frac{\nu}{M^2}\tilde{F}_3\right) + 2\frac{\varepsilon}{\tau}G_E\,\mathcal{R}\left(\delta\tilde{G}_E + \frac{\nu}{M^2}\tilde{F}_3\right) + \mathcal{O}(e^4), \tag{17}$$

where $\mathcal{R}$ stands for the real part. Comparison to results elsewhere is often facilitated by the expression

$$\frac{\nu}{M^2} = \frac{s-u}{4M^2} = \sqrt{\tau(1+\tau)\frac{1+\varepsilon}{1-\varepsilon}} . \tag{18}$$

The general expressions for the double polarization observables for an electron beam of positive helicity ($h = +1/2$) and for a recoil proton polarization along its momentum (P_l) or perpendicular, but in the scattering plane, to its momentum (P_s) can be derived as (for $m_e = 0$) [7]:

$$P_s = A_s = \tag{19}$$
$$= -\sqrt{\frac{2\varepsilon(1-\varepsilon)}{\tau}}\frac{1}{\sigma_R}\left\{G_E G_M + G_E\,\mathcal{R}\left(\delta\tilde{G}_M\right) + G_M\,\mathcal{R}\left(\delta\tilde{G}_E + \frac{\nu}{M^2}\tilde{F}_3\right) + \mathcal{O}(e^4)\right\},$$

$$P_l = -A_l = \sqrt{1-\varepsilon^2}\frac{1}{\sigma_R}\left\{G_M^2 + 2\,G_M\,\mathcal{R}\left(\delta\tilde{G}_M + \frac{\varepsilon}{1+\varepsilon}\frac{\nu}{M^2}\tilde{F}_3\right) + \mathcal{O}(e^4)\right\},$$

8

The polarizations are related to the analyzing powers A_s or A_l by time-reversal invariance, as indicated above. Note that P_l is precisely unity in the backward direction, $\varepsilon = 0$. This follows generally from lepton helicity conservation and angular momentum conservation.

An observable which is directly proportional to the two- (or multi-) photon exchange is a single-spin observable which is given by the elastic scattering of an unpolarized electron on a proton target polarized normal to the scattering plane (or the recoil polarization P_n normal to the scattering plane, which is exactly the same assuming time-reversal invariance). The corresponding single-spin asymmetry, which we refer to as the target (or recoil) normal spin asymmetry (A_n), is related to the absorptive part of the elastic eN scattering amplitude [27]. Since the one-photon exchange amplitude is purely real, the leading contribution to A_n is of order $O(e^2)$, and is due to an interference between one- and two-photon exchange amplitudes. The general expression for A_n in terms of the invariants for electron-nucleon elastic scattering is given by (in the limit $m_e = 0$),

$$P_n = A_n = \tag{20}$$
$$= \sqrt{\frac{2\,\varepsilon\,(1+\varepsilon)}{\tau}}\,\frac{1}{\sigma_R}\left\{-G_M\,\mathcal{I}\left(\delta\tilde{G}_E + \frac{\nu}{M^2}\tilde{F}_3\right) + G_E\,\mathcal{I}\left(\delta\tilde{G}_M + \left(\frac{2\varepsilon}{1+\varepsilon}\right)\frac{\nu}{M^2}\tilde{F}_3\right)\right\},$$

where $\mathcal{I}$ denotes the imaginary part.

Another single-spin observable is the normal beam asymmetry, which is discussed elsewhere [28] and which is also zero in the one-photon exchange approximation. It is proportional to the electron mass, and the asymmetry is of $\mathcal{O}(10^{-6})$ for GeV electrons. It is possibly observable in low energy elastic muon-proton scattering. It was measured in experiments at MIT/Bates and MAMI [29] at electron beam energies below 1 GeV. It is possibly also observable in low-energy elastic muon-proton scattering.

III. THE TWO-PHOTON EXCHANGE CONTRIBUTION TO ELASTIC ELECTRON-QUARK SCATTERING

In order to estimate the two-photon exchange contribution to $\tilde{G}_M$, $\tilde{F}_2$ and $\tilde{F}_3$ at large momentum transfers, we will consider a partonic calculation illustrated in Fig. 1. To begin, we calculate the subprocess on a quark, denoted by the scattering amplitude H in Fig. 1. Subsequently, we shall embed the quarks in the proton as described through the nucleon's generalized parton distributions (GPD's).
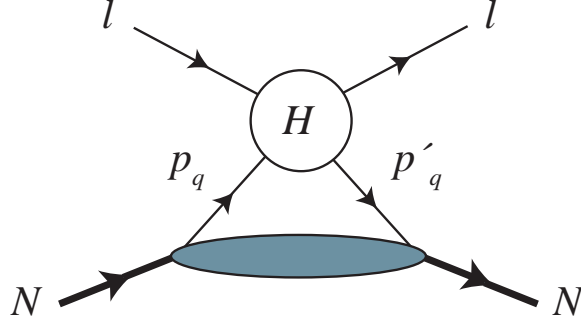
FIG. 1: Handbag approximation for the elastic lepton-nucleon scattering at large momentum transfers. In the partonic scattering process (indicated by H), the lepton scatters from quarks in the nucleon, with momenta p_q and p'_q. The lower blob represents the GPD's of the nucleon.

Elastic lepton-quark scattering,

$$l(k) + q(p_q) \rightarrow l(k') + q(p'_q) , \tag{21}$$

is described by two independent kinematical invariants, $\hat{s} \equiv (k + p_q)^2$ and $Q^2 = -t = -(k - k')^2$. We also introduce the crossing variable $\hat{u} \equiv (k - p'_q)^2$, which satisfies $\hat{s} + \hat{u} = Q^2$. The T-matrix for the two-photon part of the electron-quark scattering can be written as

$$H_{h,\lambda} = \frac{(e\,e_q)^2}{Q^2} \bar{u}(k', h)\gamma_\mu u(k, h) \cdot \bar{u}(p'_q, \lambda) \left(\tilde{f}_1 \gamma^\mu + \tilde{f}_3 \gamma.K\, P_q^\mu \right) u(p_q, \lambda), \tag{22}$$

with $P_q \equiv (p_q + p'_q)/2$, where e_q is the fractional quark charge (for a flavor q), and where $u(p_q, \lambda)$ and $u(p'_q, \lambda)$ are the quark spinors with quark helicity $\lambda = \pm 1/2$, which is conserved in the scattering process for massless quarks. Quark helicity conservation leads to the absence of any analog of $\tilde{F}_2$ in the general expansion of Eq. (12).

In order to calculate the partonic scattering helicity amplitudes $H_{h,\lambda}$ of Eq. (22) at order $O(e^4)$, we consider the two-photon exchange direct and crossed box diagrams of Fig. 2. The two-photon exchange contribution to the elastic electron-scattering off spin 1/2 Dirac particles was first calculated in Ref. [30], which we verified explicitly. For further use, we separate the amplitude $\tilde{f}_1$ for the scattering of massless electrons off massless quarks into a soft and hard part, i.e. $\tilde{f}_1 = \tilde{f}_1^{soft} + \tilde{f}_1^{hard}$. The soft part corresponds with the situation where one of the photons in Fig. 2 carries zero four-momentum, and is obtained by replacing the other photon's four-momentum by q in both numerator and denominator of the loop
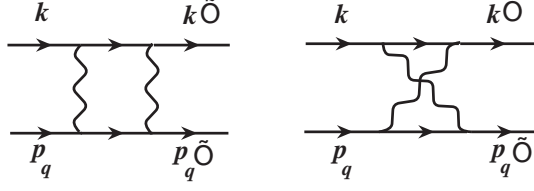
10

FIG. 2: Direct and crossed box diagrams to describe the two-photon exchange contribution to the lepton-quark scattering process, corresponding with the blob denoted by H in Fig. 1.

integral [31]. This yields,

$$\mathcal{R}\left(\tilde{f}_1^{soft}\right) = \frac{e^2}{4\pi^2}\left\{\ln\left(\frac{\lambda^2}{\sqrt{-\hat{s}\hat{u}}}\right)\ln\left|\frac{\hat{s}}{\hat{u}}\right| + \frac{\pi^2}{2}\right\},\tag{23}$$

$$\mathcal{R}\left(\tilde{f}_1^{hard}\right) = \frac{e^2}{4\pi^2}\left\{\frac{1}{2}\ln\left|\frac{\hat{s}}{\hat{u}}\right| + \frac{Q^2}{4}\left[\frac{1}{\hat{u}}\ln^2\left|\frac{\hat{s}}{Q^2}\right| - \frac{1}{\hat{s}}\ln^2\left|\frac{\hat{u}}{Q^2}\right| - \frac{1}{\hat{s}}\pi^2\right]\right\},\tag{24}$$

where $\tilde{f}_1^{soft}$, which contains a term proportional to $\ln\lambda^2$ (λ is an infinitesimal photon mass), is IR divergent. The amplitude $\tilde{f}_3$ resulting from the diagrams of Fig. 2 is IR finite, and its real part is

$$\mathcal{R}\left(\tilde{f}_3\right) = \frac{e^2}{4\pi^2}\frac{1}{\hat{s}\,\hat{u}}\left\{\hat{s}\,\ln\left|\frac{\hat{s}}{Q^2}\right| + \hat{u}\,\ln\left|\frac{\hat{u}}{Q^2}\right| + \frac{\hat{s}-\hat{u}}{2}\left[\frac{\hat{s}}{\hat{u}}\ln^2\left|\frac{\hat{s}}{Q^2}\right| - \frac{\hat{u}}{\hat{s}}\ln^2\left|\frac{\hat{u}}{Q^2}\right| - \frac{\hat{u}}{\hat{s}}\pi^2\right]\right\}.\tag{25}$$

The correction to the electron-quark elastic cross section can be obtained from Eq. (17),

$$d\sigma = d\sigma_{1\gamma}\left[1 + 2\,\mathcal{R}\left(\tilde{f}_1\right)_{2\gamma} + \varepsilon\,\frac{\hat{s}-\hat{u}}{4}\,2\,\mathcal{R}\left(\tilde{f}_3\right)_{2\gamma}\right],$$
$$\equiv d\sigma_{1\gamma}\left(1 + \delta_{2\gamma}\right),\tag{26}$$

where $d\sigma_{1\gamma}$ is the cross section in the one-photon exchange approximation and $\varepsilon = -2\,\hat{s}\,\hat{u}\,/\,(\hat{s}^2 + \hat{u}^2)$ in the massless limit. Using Eqs. (23, 24, 25), we obtain (for $e_q = +1$)

$$\delta_{2\gamma} = \frac{e^2}{4\pi^2}\left\{2\ln\left(\frac{\lambda^2}{Q^2}\right)\ln\left|\frac{\hat{s}}{\hat{u}}\right|\right.\tag{27}$$
$$\left. + \frac{(\hat{s}-\hat{u})Q^2}{2\,(\hat{s}^2+\hat{u}^2)}\left[\ln^2\left|\frac{\hat{s}}{Q^2}\right| + \ln^2\left|\frac{\hat{u}}{Q^2}\right| + \pi^2\right] + \frac{Q^4}{\hat{s}^2+\hat{u}^2}\left[\frac{\hat{u}}{Q^2}\ln\left|\frac{\hat{s}}{Q^2}\right| - \frac{\hat{s}}{Q^2}\ln\left|\frac{\hat{u}}{Q^2}\right|\right]\right\},$$

which is in agreement with the corresponding expression for electron-muon scattering obtained in Ref. [32]. The expressions of $\tilde{f}_1$ and $\tilde{f}_3$ can also be obtained through crossing from the corresponding expressions of the box diagrams for the process $e^+e^- \rightarrow \mu^+\mu^-$ as calculated in Ref. [33].

11

We will need the expressions for the imaginary parts of $\tilde{f}_1$ and $\tilde{f}_3$ in order to calculate the normal spin asymmetry A_n. These imaginary parts originate solely from the direct two-photon exchange box diagram of Fig. 2 and are given by

$$\mathcal{I}\left(\tilde{f}_1^{soft}\right) = -\frac{e^2}{4\pi}\ln\left(\frac{\lambda^2}{\hat{s}}\right), \tag{28}$$

$$\mathcal{I}\left(\tilde{f}_1^{hard}\right) = -\frac{e^2}{4\pi}\left\{\frac{Q^2}{2\,\hat{u}}\ln\left(\frac{\hat{s}}{Q^2}\right) + \frac{1}{2}\right\}, \tag{29}$$

$$\mathcal{I}\left(\tilde{f}_3\right) = -\frac{e^2}{4\pi}\frac{1}{\hat{u}}\left\{\frac{\hat{s}-\hat{u}}{\hat{u}}\ln\left(\frac{\hat{s}}{Q^2}\right) + 1\right\}. \tag{30}$$

Notice that the IR divergent part in Eq. (28) does not contribute when calculating the normal spin asymmetry A_n of Eq. (20). Indeed at the quark level, one may complete the calculation for quark mass m_q nonzero and find that A_n is given by,

$$A_n = \frac{e_q e^2}{4\pi}\frac{m_q}{2\,Q}\frac{\sqrt{2\varepsilon(1+\varepsilon)}}{1+4\varepsilon m_q^2/Q^2}\frac{Q^2(Q^2+4m_q^2)}{\hat{s}(\hat{s}-\hat{u})} \tag{31}$$

an IR finite quantity (*cf.* [34]).

IV. THE HANDBAG CALCULATION OF THE TWO-PHOTON EXCHANGE CONTRIBUTION TO ELASTIC ELECTRON-NUCLEON SCATTERING

Having calculated the partonic subprocess, we next discuss how to embed the quarks in the nucleon. We begin by discussing the soft contributions. The handbag diagrams discussed so far have both photons coupled to the same quark. There are also contributions from processes where the photons interact with different quarks. One can show that the IR contributions from these processes, which are proportional to the products of the charges of the interacting quarks, added to the soft contributions from the handbag diagrams give the same result as the soft contributions calculated with just a nucleon intermediate state [35]. Thus the low energy theorem for Compton scattering is satisfied. As discussed in the introduction, the hard parts which appear when the photons couple to different quarks, the so-called cat's ears diagrams, are neglected in the handbag approximation.

For the real parts, the IR divergence arising from the direct and crossed box diagrams, at the nucleon level, is cancelled when adding the bremsstrahlung contribution from the interference of diagrams where a soft photon is emitted from the electron and from the

proton. This provides a radiative correction term from the soft part of the boxes plus electron-proton bremsstrahlung which added to the lowest order term may be written as

$$\sigma_{soft} = \sigma_{1\gamma} \left(1 + \delta_{2\gamma, soft} + \delta_{brems}^{ep}\right), \tag{32}$$

where $\sigma_{1\gamma}$ is the one-photon exchange cross section. In Eq. (32), the soft-photon contribution due to the nucleon box diagram is given by

$$\delta_{2\gamma, soft} = \frac{e^2}{2\pi^2} \left\{ \ln \left(\frac{\lambda^2}{\sqrt{(s - M^2)|u - M^2|}} \right) \ln \left| \frac{s - M^2}{u - M^2} \right| \tag{33} \right.$$
$$\left. - L \left(\frac{s - M^2}{s} \right) - \frac{1}{2} \ln^2 \left(\frac{s - M^2}{s} \right) + \mathcal{R} \left[L \left(\frac{u - M^2}{u} \right) \right] + \frac{1}{2} \ln^2 \left(\frac{u - M^2}{u} \right) + \frac{\pi^2}{2} \right\},$$

where L is the Spence function defined by

$$L(z) = - \int_0^z dt \, \frac{\ln(1 - t)}{t} . \tag{34}$$

The bremsstrahlung contribution where a soft photon is emitted from an electron and proton line (*i.e.*, by cutting one of the (soft) photon lines in Fig. 2) was calculated in Ref. [10], which we verified explicitly, and is for the case that the outgoing electron is detected,

$$\delta_{brems}^{ep} = \frac{e^2}{2\pi^2} \left\{ \ln \left(\frac{4 (\Delta E)^2 (s - M^2)^2}{\lambda^2 y (u - M^2)^2} \right) \ln \left(\frac{s - M^2}{M^2 - u} \right) \right.$$
$$\left. + L \left(1 - \frac{1}{y} \frac{s - M^2}{M^2 - u} \right) - L \left(1 - \frac{1}{y} \frac{M^2 - u}{s - M^2} \right) \right\}, \tag{35}$$

where $\Delta E \equiv E_e^{'el} - E_e^{'}$ is the difference of the measured outgoing electron *lab* energy ($E_e^{'}$) from its elastic value ($E_e^{'el}$), and $y \equiv (\sqrt{\tau} + \sqrt{1 + \tau})^2$. One indeed verifies that the sum of Eqs. (33,35) is IR finite. When comparing with elastic ep cross section data, which are usually radiatively corrected using the procedure of Mo and Tsai, Ref. [8], we have to consider only the difference of our $\delta_{2\gamma, soft} + \delta_{brems}^{ep}$ relative to the $\mathcal{O}(Z^2)$ part, in their notation, of the radiative correction in [8]. Except for the $\pi^2/2$ term in Eq. (33), this difference was found to be below 10^{-3} for all kinematics considered in Fig. 3.

Having discussed the two-photon exchange contribution on the nucleon when one of the two photons is soft, we next discuss the contribution which arises from the hard part (that is, neither photons soft) of the partonic amplitude coming from the box diagrams. This part of the amplitude is calculated, in the kinematical regime where s, $-u$, and Q^2 are large compared to a hadronic scale ($s, -u, Q^2 >> M^2$), as a convolution between a hard scattering

13

electron-quark amplitude and a soft matrix element on the nucleon. It is convenient to choose a frame where $q^+ = 0$, as in [36], where we introduce light-cone variables $a^\pm \propto (a^0 \pm a^3)$ and choose the z-axis along the direction of P^3 (so that P has a large + component). We use the symmetric frame, as in [19], where the external momenta and q are

$$
\begin{aligned}
k &= \left[\eta P^+, \frac{1}{P^+} \frac{Q^2}{4\eta}, \frac{1}{2} \vec{q}_\perp \right] , \\
k' &= \left[\eta P^+, \frac{1}{P^+} \frac{Q^2}{4\eta}, -\frac{1}{2} \vec{q}_\perp \right] , \\
q &= [0, 0, \vec{q}_\perp] , \\
p &= \left[P^+, \frac{1}{P^+} \left(M^2 + \frac{Q^2}{4} \right), -\frac{1}{2} \vec{q}_\perp \right] , \\
p' &= \left[P^+, \frac{1}{P^+} \left(M^2 + \frac{Q^2}{4} \right), \frac{1}{2} \vec{q}_\perp \right] .
\end{aligned}
\tag{36}
$$

Then,

$$
s = \frac{(1+\eta)^2}{4\eta} Q^2 + (1+\eta) M^2 , \qquad u = -\frac{(1-\eta)^2}{4\eta} Q^2 + (1-\eta) M^2 ,
\tag{37}
$$

one may check that $s + u = 2M^2 + Q^2$ and also solve for the lepton light-front momentum fractions, $\eta = k^+/P^+ = k'^+/P^+$, as

$$
\eta = \frac{1}{Q^2 + 4 M^2} \left[s - u - 2 \sqrt{M^4 - s u} \right] .
\tag{38}
$$

For comparison, forward scattering in the CM, $\theta_{\mathrm{CM}} = 0°$, matches to $\eta = 0$ and backward scattering, $\theta_{\mathrm{CM}} = 180°$, matches to $\eta = (s - M^2)/s$.

In the $q^+ = 0$ frame, the parton light-front momentum fractions are defined as $x = p_q^+/P^+ = p_q'^+/P^+$. The active partons, on which the hard scattering takes place, are approximately on-shell. In the symmetric frame, we take the spectator partons to have transverse momenta that are small (relative to P) and can be neglected when evaluating the hard scattering amplitude H in Fig. 1. The Mandelstam variables for the process (21) on the quark, which enter in the evaluation of the hard scattering amplitude, are then given by

$$
\hat{s} = \frac{(x+\eta)^2}{4 x \eta} Q^2 , \qquad \hat{u} = -\frac{(x-\eta)^2}{4 x \eta} Q^2 .
\tag{39}
$$

Note that in the limit $x \simeq 1$, where $\hat{s} \simeq s$ and $\hat{u} \simeq u$, the quark momenta are collinear with their parent hadron momenta, i.e. $p_q \simeq p$ and $p_q' \simeq p'$. This is the simplest situation for the handbag approximation, in which it was shown possible to factorize the wide angle real

14

Compton scattering amplitude in terms of a hard scattering process and a soft overlap of hadronic light-cone wave functions, which in turn can be expressed as moments of generalized parton distributions (GPD's) [19, 20]. In the following we will extend the handbag [19, 37] formalism to calculate the two-photon exchange amplitude to elastic electron-nucleon scattering at moderately large momentum transfers, and derive the amplitude within a more general unfactorized framework by keeping the x dependence in the hard scattering amplitude (*i.e.*, by not taking the $x \to 1$ limit from the outset).

For the process (5) in the kinematical regime $s, -u, Q^2 >> M^2$, the (unfactorized) hand-bag approximation implies that the T-matrix can be written as[2]

$$T^{hard}_{h, \lambda'_N \lambda_N} = \int_{-1}^{1} \frac{dx}{x} \sum_q \frac{1}{2} \left[H^{hard}_{h, +\frac{1}{2}} + H^{hard}_{h, -\frac{1}{2}} \right] \times \tag{40}$$

$$\times \frac{1}{2} \left[H^q \left(x, 0, q^2 \right) \bar{u}(p', \lambda'_N) \gamma \cdot n \, u(p, \lambda_N) + E^q \left(x, 0, q^2 \right) \bar{u}(p', \lambda'_N) \frac{i \, \sigma^{\mu\nu} \, n_\mu q_\nu}{2M} u(p, \lambda_N) \right]$$

$$+ \int_{-1}^{1} \frac{dx}{x} \sum_q \frac{1}{2} \left[H^{hard}_{h, +\frac{1}{2}} - H^{hard}_{h, -\frac{1}{2}} \right] \cdot \frac{1}{2} \text{sgm}(x) \, \tilde{H}^q \left(x, 0, q^2 \right) \bar{u}(p', \lambda'_N) \gamma \cdot n \, \gamma_5 \, u(p, \lambda_N),$$

where the hard scattering amplitude H^{hard} is evaluated using the hard part of $\tilde{f}_1$ and $\tilde{f}_3$, with kinematics $\hat{s}$ and $\hat{u}$ according to Eq. (39), and where n^μ is a Sudakov four-vector ($n^2 = 0$), which can be expressed as

$$n^\mu = \frac{2}{\sqrt{M^4 - su}} \left\{ -\eta \, P^\mu + K^\mu \right\}. \tag{41}$$

Furthermore in Eq. (40), $H^q, E^q, \tilde{H}^q$ are the GPD's for a quark q in the nucleon (for a review see, *e.g.*, Ref. [38]).

¿From Eqs. (12), (22), and (40) the hard 2γ exchange contributions to $\delta\tilde{G}_M$, $\delta\tilde{G}_E$, and $\tilde{F}_3$ are obtained (after some algebra) as

$$\delta\tilde{G}^{hard}_M = C, \tag{42}$$

$$\delta\tilde{G}^{hard}_E = -\left(\frac{1+\varepsilon}{2\varepsilon} \right) (A - C) + \sqrt{\frac{1+\varepsilon}{2\varepsilon}} \, B, \tag{43}$$

$$\tilde{F}_3 = \frac{M^2}{\nu} \left(\frac{1+\varepsilon}{2\varepsilon} \right) (A - C), \tag{44}$$

---

[2] The corresponding equation in Ref. [13] contains typographical errors regarding factors of (1/2). The remaining equations in that paper are written correctly.

with

$$A \equiv \int_{-1}^{1} \frac{dx}{x} \frac{\left[(\hat{s} - \hat{u}) \tilde{f}_1^{hard} - \hat{s}\hat{u}\tilde{f}_3 \right]}{(s - u)} \sum_q e_q^2 \left(H^q + E^q \right),$$

$$B \equiv \int_{-1}^{1} \frac{dx}{x} \frac{\left[(\hat{s} - \hat{u}) \tilde{f}_1^{hard} - \hat{s}\hat{u}\tilde{f}_3 \right]}{(s - u)} \sum_q e_q^2 \left(H^q - \tau E^q \right),$$

$$C \equiv \int_{-1}^{1} \frac{dx}{x} \tilde{f}_1^{hard} \, \text{sgm}(x) \sum_q e_q^2 \, \tilde{H}^q, \tag{45}$$

where note that in Eqs. (42)-(44), the partonic amplitude $\tilde{f}_1$ has its soft IR divergent part removed as discussed before.

Equations (42)-(44) reduce to the partonic amplitudes in the limit $M \to 0$ by considering a quark target for which the GPD's are given by,

$$H^q \rightarrow \delta(1 - x),$$

$$E^q \rightarrow 0,$$

$$\tilde{H}^q \rightarrow \delta(1 - x). \tag{46}$$

In this limit, and using the identity

$$-\frac{\hat{s}\hat{u}}{\hat{s} - \hat{u}} = \frac{\hat{s} - \hat{u}}{4} \frac{2\varepsilon}{1 + \varepsilon}, \tag{47}$$

we find that

$$\delta\tilde{G}_M^{hard} \rightarrow \sum_q e_q^2 \tilde{f}_1^{hard},$$

$$\frac{\delta\tilde{F}_2}{M} \rightarrow 0,$$

$$\frac{\delta\tilde{F}_3}{M^2} \rightarrow \sum_q e_q^2 \tilde{f}_3. \tag{48}$$

¿From the integrals A, B, and C, and the usual form factors, we can directly construct the observables. The cross section is

$$\sigma_R = \sigma_{R,soft} + \sigma_{R,hard}, \tag{49}$$

where

$$\sigma_{R,hard} = (1 + \varepsilon) \, G_M \, \mathcal{R}(A) + \sqrt{2\varepsilon(1 + \varepsilon)} \frac{1}{\tau} \, G_E \, \mathcal{R}(B) + (1 - \varepsilon) \, G_M \, \mathcal{R}(C). \tag{50}$$

16

¿From Eqs. (32) to (35) and the discussion surrounding them, we learned that to a good approximation the result for the soft part can be written as

$$\sigma_{R,soft} = \sigma_{R,1\gamma} \left(1 + \pi\alpha + \delta^{MT}\right) , \qquad (51)$$

where δ^{MT} is the correction given in Ref. [8]. Since the data is very commonly corrected using [8], let us define $\sigma_R^{MT\ corr} \equiv \sigma_R/(1 + \delta^{MT})$. Then an accurate relationship between the data with Mo-Tsai corrections already included and the form factors is

$$\sigma_R^{MT\ corr} = \left(G_M^2 + \frac{\varepsilon}{\tau}G_E^2\right)(1 + \pi\alpha) + \sigma_{R,hard} , \qquad (52)$$

where the extra terms on the right-hand-side come from two-photon exchange and $\mathcal{O}(e^4)$ terms are not included. The reader may marginally improve the expression by including with the $(1+\pi\alpha)$ factor the circa 0.1% difference between our actual soft results and those of [8]; from our side the relevant formulas are the aforementioned (32) to (35). Since the Mo-Tsai corrections are so commonly made in experimental papers before reporting the data, the "$MT\ corr$" superscript will be understood rather than explicit when we show cross section plots below. Finally, before discussing polarization, the fact that a $\pi^2/2$ term, or $(\pi\alpha)$ term after multiplying in the overall factors, sits in the soft corrections has to do with the specific criterion we used, that of Ref. [31], to separate the soft from hard parts. The term cannot be eliminated; with a different criterion, however, that term can move into the hard part.

The double polarization observables of Eqs. (53,54) are given by

$$P_s = -\sqrt{\frac{2\varepsilon(1-\varepsilon)}{\tau}} \frac{1}{\sigma_R} \left\{ G_E G_M + G_E \mathcal{R}\left(C\right) + G_M \sqrt{\frac{1+\varepsilon}{2\varepsilon}} \mathcal{R}\left(B\right) + \mathcal{O}(e^4) \right\}, \quad (53)$$

$$P_l = \sqrt{1-\varepsilon^2} \frac{1}{\sigma_R} \left\{ G_M^2 + G_M \mathcal{R}\left(A+C\right) + \mathcal{O}(e^4) \right\}, \qquad (54)$$

and the target normal spin asymmetry of Eq. (20) is

$$A_n = \sqrt{\frac{2\varepsilon\left(1+\varepsilon\right)}{\tau}} \frac{1}{\sigma_R} \left\{ G_E \mathcal{I}\left(A\right) - \sqrt{\frac{1+\varepsilon}{2\varepsilon}} G_M \mathcal{I}\left(B\right) \right\}, \qquad (55)$$

One sees from Eq. (55) that A_n does not depend on the GPD $\tilde{H}$.

We will need to specify a model for the GPD's in order to estimate the crucial integrals Eqs. (45) for the two-photon exchange amplitudes We will present results from two different GPD models: a gaussian model and a modified Regge model.

First, following Ref. [20], we use a gaussian valence model which is unfactorized in x and Q^2 for the GPD's H and $\tilde{H}$,

$$H^q(x, 0, q^2) = q_v(x) \, \exp\left(-\frac{(1-x)\,Q^2}{4\,x\,\sigma}\right), \tag{56}$$

$$\tilde{H}^q(x, 0, q^2) = \Delta q_v(x) \, \exp\left(-\frac{(1-x)\,Q^2}{4\,x\,\sigma}\right), \tag{57}$$

where $q_v(x)$ is the valence quark distribution and $\Delta q_v(x)$ the polarized valence quark distribution. In the following estimates we take the unpolarized parton distributions at input scale $Q_0^2 = 1$ GeV^2 from the MRST2002 global NNLO fit [39] as

$$u_v = 0.262\, x^{-0.69}(1-x)^{3.50}\left(1 + 3.83\, x^{0.5} + 37.65\, x\right),$$

$$d_v = 0.061\, x^{-0.65}(1-x)^{4.03}\left(1 + 49.05\, x^{0.5} + 8.65\, x\right).$$

For the polarized parton distributions, we adopt the recent NLO analysis of Ref. [40], which at input scale $Q_0^2 = 1$ GeV^2 yields

$$\Delta u_v = 0.505 x^{-0.33}(1-x)^{3.428}\left(1 + 2.179 x^{0.5} + 14.57 x\right),$$

$$\Delta d_v = -0.0185 x^{-0.73}(1-x)^{3.864}\left(1 + 35.47 x^{0.5} + 28.97 x\right).$$

For the GPD E, whose forward limit is unknown, we adopt a valence parametrization multiplied with $(1-x)^2$ to be consistent with the $x \to 1$ limit [41]. This gives

$$E^q(x, 0, q^2) = \frac{\kappa^q}{N^q}(1-x)^2 q_v(x) \exp\left(-\frac{(1-x)Q^2}{4\,x\,\sigma}\right), \tag{58}$$

where the normalization factors $N^u = 1.377$ and $N^d = 0.7554$ are chosen in such a way that the first moments of E^u and E^d at $Q^2 = 0$ yield the anomalous magnetic moments $\kappa^u = 2\kappa^p + \kappa^n = 1.673$ and $\kappa^d = \kappa^p + 2\kappa^n = -2.033$ respectively. Furthermore, the parameter σ in Eqs. (56,57,58) is related to the average transverse momentum of the quarks inside the nucleon by $\sigma = 5 < k_\perp^2 >$. Its value has been estimated in Ref. [19] as $\sigma \simeq 0.8$ GeV^2, which we will adopt in the following calculations.

The GPD's just described were used in our shorter note [13]. Recently, GPD's whose first moments give a better account of the nucleon form factors have become available [42]. These GPD's we refer to as a modified Regge model [42], and entail

$$H^q(x, 0, q^2) = q_v(x) \, x^{a_1'(1-x)Q^2} \,,$$

$$E^q(x, 0, q^2) = \frac{\kappa^q}{N^q}(1-x)^{\eta_q} q_v(x) \, x^{a_2'(1-x)Q^2} \,,$$

$$\tilde{H}^q(x, 0, q^2) = \Delta q_v(x) \, x^{\tilde{a}_1'(1-x)Q^2} \,. \tag{59}$$

18

We still use the same q_v and the same Δq_v as given above. The five parameters are

$$\alpha_1' = 1.098 \text{ GeV}^{-2}, \qquad \alpha_2' = 1.158 \text{ GeV}^{-2}, \qquad \tilde{\alpha}_1' = 1.000 \text{ GeV}^{-2},$$

$$\eta_u = 1.52, \qquad \eta_d = 0.31, \tag{60}$$

and the normalization factors here become $N_u = 1.519$ and $N_d = 0.9447$. The modified Regge GPD's formally do not give convergence at low Q^2 for integrands with negative powers of x, such as we have here (or as one finds in [19]). The integrals could be defined by analytically continuing in the Regge intercept [17, 18]. We will use them only for $Q^2 \geq 2$ GeV^2, and all the integrals converge straightforwardly.

We shall investigate in forthcoming plots the sensitivity of the results to the two GPD's.

V. RESULTS

A. Cross section

In Fig. 3, we display the effect of 2γ exchange on the reduced cross section σ_R, as given in Eq. (17), for electron-proton scattering. For the form factor ratio, we always use G_E^p/G_M^p as extracted from the polarization transfer experiments [2].

We should remind the reader that G_M^p is also obtained from the reduced cross section data: the normalization gives G_M^p and the slope gives G_E^p/G_M^p. As a starting point we adopt the parametrization for G_M^p, of Ref. [43]. The straight dotted curves of Fig. 3 show that the values of G_E^p/G_M^p extracted from the polarization experiments are inconsistent with the one-photon exchange analysis of the Rosenbluth data, corrected with just the classic Mo and Tsai radiative corrections [8], in the Q^2 range where data from both methods exist. We then include the 2γ exchange correction, using the GPD based calculation described in this paper. The plots show the results from both the GPD's used in our shorter note [13] and recorded in the previous section, as well as from the alternative GPD's also described in the previous section. The results are rather similar.

It is also important to note the non-linearity in the Rosenbluth plot, particularly at the largest ε values. One sees that over most of the ε range, the overall slope has become steeper, in agreement with the experimental data. This change in slope is crucial: we see that including the 2γ exchange allows one to reconcile the polarization transfer and Rosenbluth data.
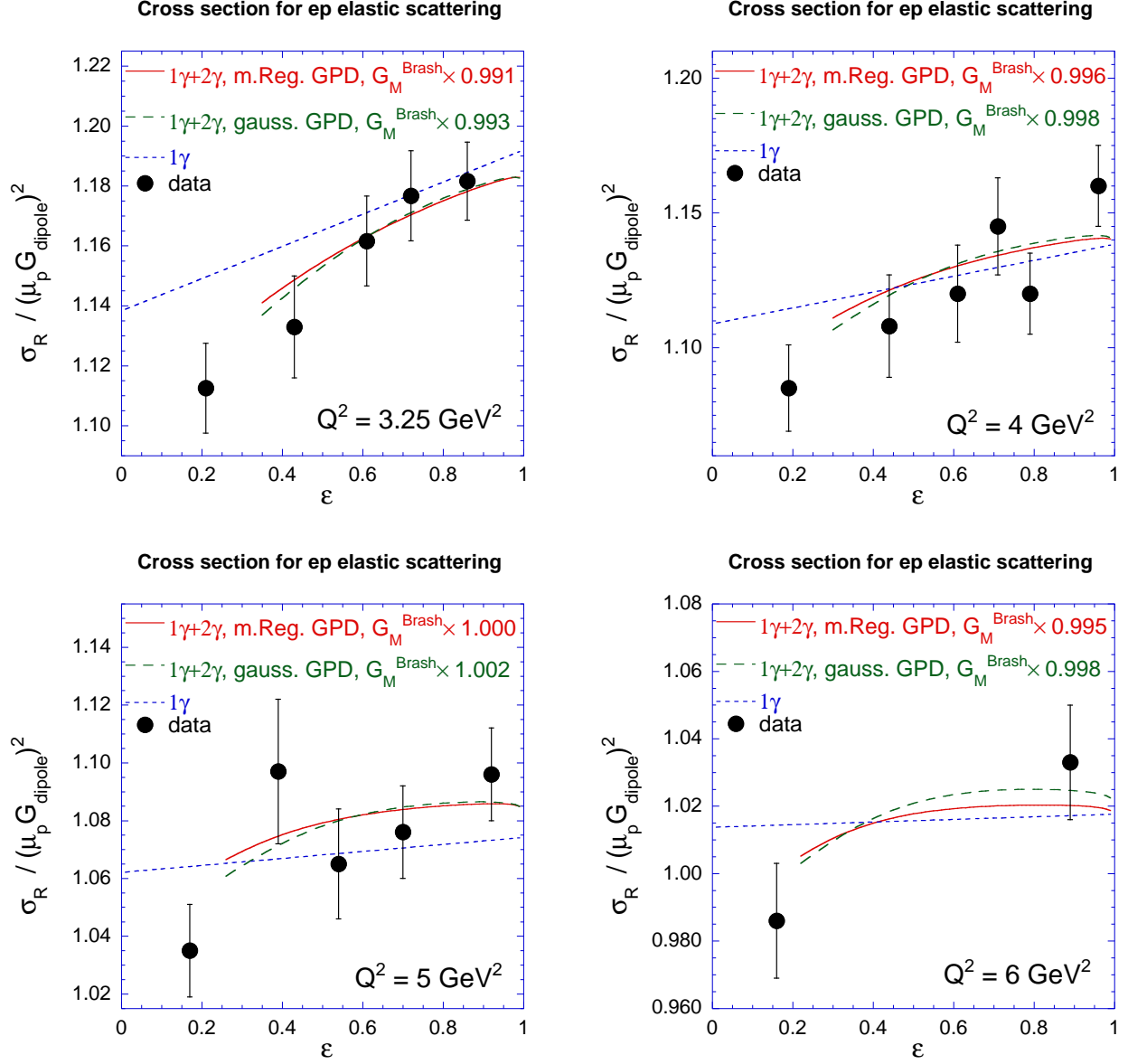
19

FIG. 3: Rosenbluth plots for elastic ep scattering: σ_R divided by $(\mu_p G_D)^2$, with $G_D = (1 + Q^2/0.71)^{-2}$. Dotted curves: Born approximation using G_{Ep}/G_{Mp} from polarization data [1, 2]. Solid curves: full calculation using the modified Regge GPD, for the kinematical range $-u > M^2$. Dashed curves: same as solid curves but using the gaussian GPD. The data are from Ref. [6].

It is clearly worthwhile to do a global re-analysis of all large Q^2 elastic data including the 2γ exchange correction in order to redetermine the values of G_E^p and G_M^p. For example, in order to best fit the data when including the 2γ exchange correction, one should slightly change the value of G_M^p of Ref. [43]. A full analysis is beyond the scope of this paper,

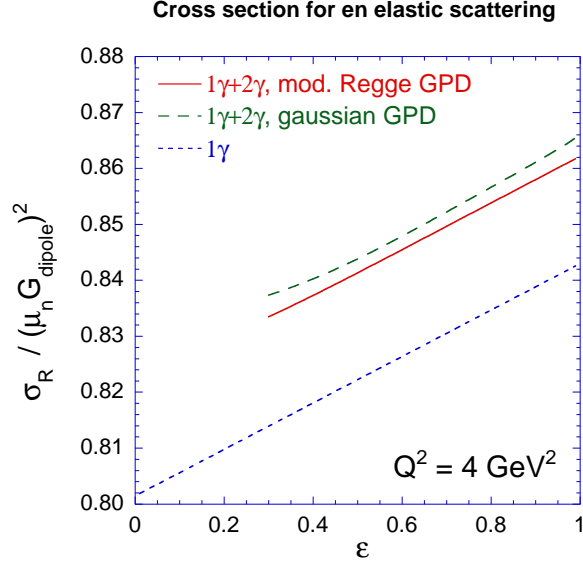In Fig. 4, we show a similar plot for electron-neutron elastic scattering. Because of

20

Cross section for en elastic scattering

FIG. 4: A Rosenbluth plot for elastic en scattering. The curves with the two-photon corrections are plotted only for $-u > M^2$. For G_M^n and G_E^n we used fits from [44] and [45], respectively. There is little slope change for the neutron case, for reasons noted in the text.

a partial cancellation between contributions proportional to G_E^n and G_M^n, there is little ε dependence in the corrections, and the slope is not appreciably modified. We took G_M^n from the fit of [44]; for G_E^n we used the fit given in [45].

B. Single spin asymmetry

The single spin asymmetry A_n or P_n is a direct measure of the imaginary part of the 2γ exchange amplitudes. Our GPD estimate for A_n for the proton is shown in the left-hand plot of Fig. 5 as a function of the CM scattering angle for fixed incoming electron lab energy, taken here as 6 GeV. Also shown is a calculation of A_n including the elastic intermediate state only [27]. The result, which is nearly the same for either of the two GPD's that we use, is of order 1%.

Fig. 5 on the right also shows a similar plot of the single spin asymmetry for a neutron target. The predicted asymmetry is of opposite sign, reflecting that the numerically largest term is the one proportional to G_M. The results are again of order 1% in magnitude, though somewhat larger for the neutron than for the proton.

A precision measurement of A_n is planned at JLab [46] on a polarized ^3He target; it

Normal Polarization or Analyzing Power - Proton

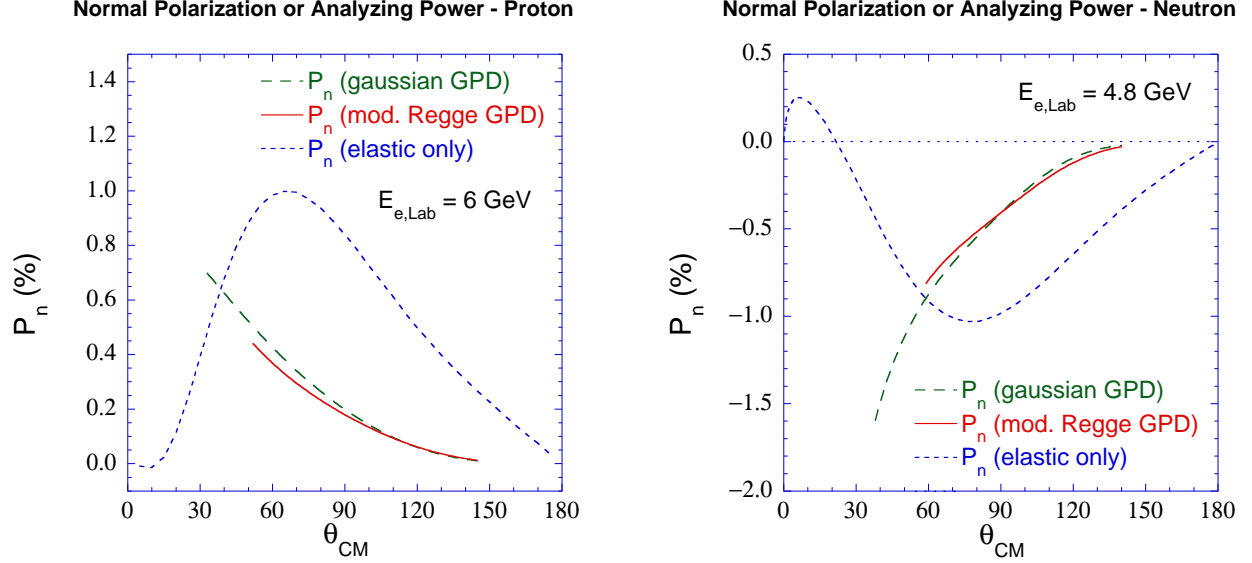**Normal Polarization or Analyzing Power - Neutron**

FIG. 5: Nucleon analyzing power, which is equal to normal recoil polarization. The elastic contribution (nucleon intermediate state in the two-photon exchange box diagram) is shown by the dotted curve [27]. The GPD calculation for the inelastic contribution is shown by the dashed curve for the gaussian GPD, and by the solid curve for the modified Regge GPD. The GPD calculation is cut off in the backward direction at $-u = M^2$. In the forward direction the modified Regge GPD result goes down to $Q^2 = 2$ GeV^2 and the gaussian GPD result to $Q^2 = M^2$.

will provide access to the elastic electron-neutron single-spin asymmetry from two-photon exchange.

C. Polarization transfers

The polarization transfer method for measuring the ratio G_E/G_M depends on measuring outgoing nucleon polarizations P_l and P_s for polarized incoming electrons. Their ratio is

$$\frac{P_s}{P_l} = -\sqrt{\frac{2\epsilon}{\tau(1+\epsilon)}} \frac{G_E}{G_M} , \tag{61}$$

in the one-photon exchange calculation. This also is subject to additional corrections from two-photon exchange. However, the impact of the corrections upon G_E is not in any way enhanced, and so one expects and finds that the corrections to G_E measured this way are smaller than the corrections to G_E coming from the cross section experiments.

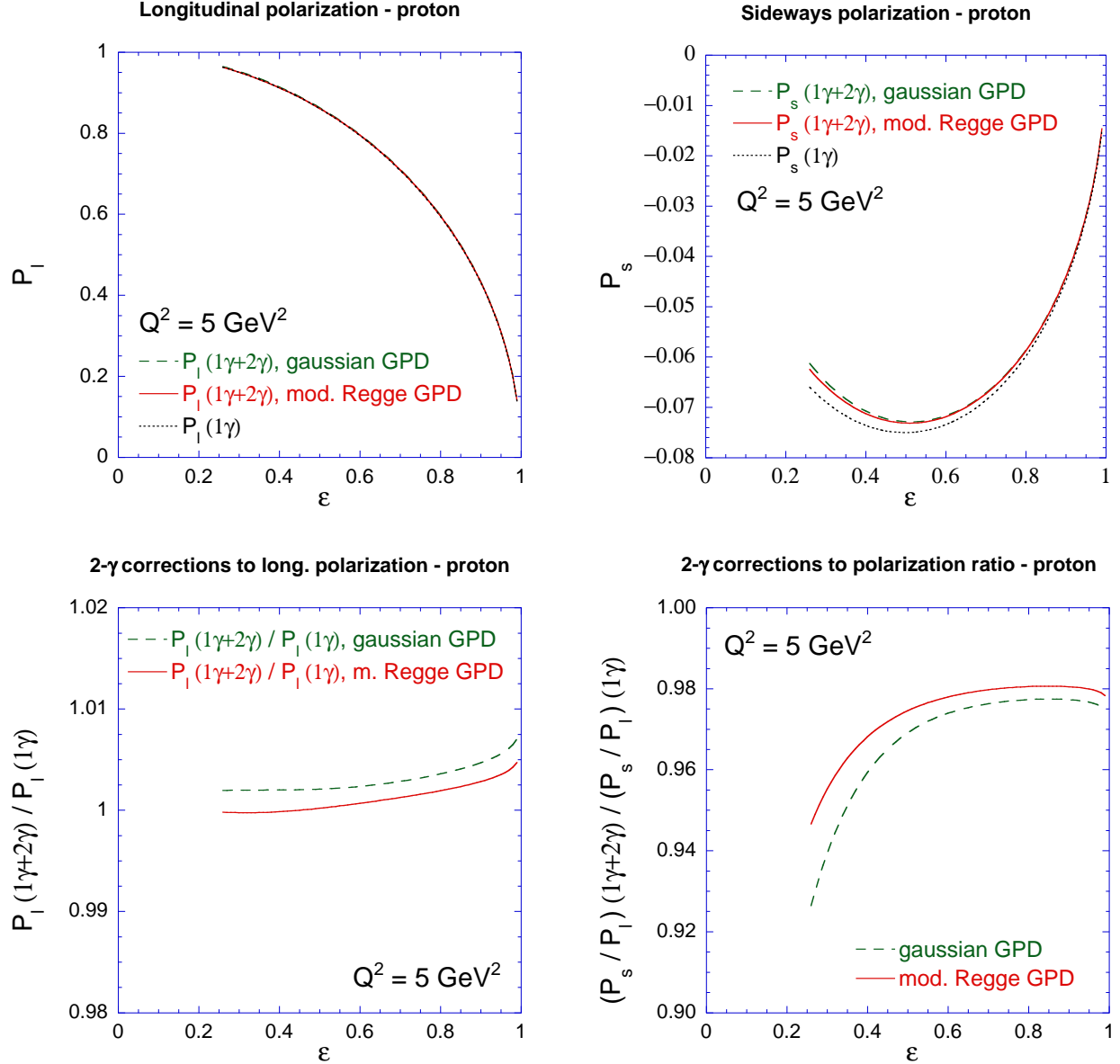Figure 6 shows in the upper two panels the calculated P_l and P_s for ep scattering with

FIG. 6: Recoil proton polarization components P_s and P_l and their ratios relative to the 1γ exchange results (lower panels) for elastic ep scattering at $Q^2 = 5$ GeV^2. The dotted curves in the upper panels are the Born approximation (1γ exchange) results. The solid curves include the 2γ exchange correction using the GPD calculation, for the kinematical range where both $s, -u > M^2$.

and without the two-photon exchange terms, for 100% right-handed electron polarization and with fixed momentum transfer $Q^2 = 5$ GeV^2. The two GPD's were presented in the previous section, and we use again the polarization G_E/G_M from [2] and G_M from [43]. The corrections to the longitudinal polarization are quite small, as is seen again in the lower left panel, where the ratio of the full calculation divided by the one-photon exchange calculation
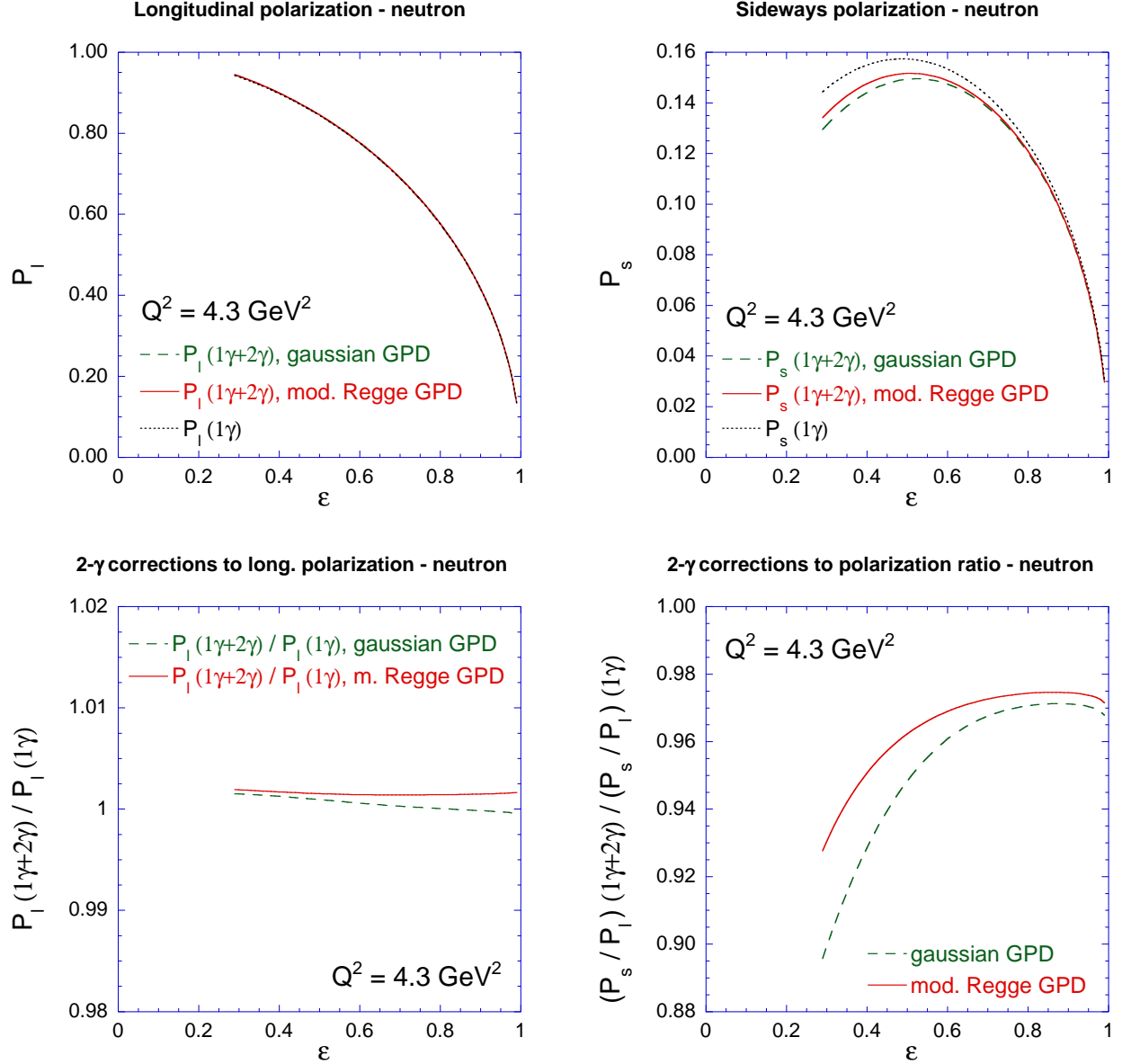
FIG. 7: Recoil neutron polarization components P_s and P_l and their ratios relative to the 1γ exchange results (lower panels) for elastic ep scattering at $Q^2 = 4.3$ GeV^2. See Fig. 6 for notation.

is shown. The lower right panel shows the corrections to the P_s/P_l ratio, given as a ratio again of the full calculation to the one-photon calculation. An experiment to measure the ε-dependence of P_s/P_l is planned at JLab [47]. This will allow a test of the two-photon corrections.

Figure 7 shows the corresponding plots for the neutron, at a momentum transfer squared of 4.3 GeV^2. If one needs to choose between the GPD's, the modified Regge model should be chosen as it gives the better account of the existing data on the form factors, the neutron

form factors in particular [42].

D. Positron-proton vs. electron-proton

Positron-proton and electron-proton scattering have the opposite sign for the two-photon corrections relative to the one-photon terms. Hence one expects e^+p and e^-p elastic scattering to differ by a few percent. Figure 8 shows our results for three different Q^2 values. These curves are obtained by adding our two-photon box calculation, minus the corresponding part of the soft only calculation in [8], to the one-photon calculations; hence, they are meant to be compared to data where the corrections given in [8] have already been made. Each curve is based on the gaussian GPD and is cut off at low ε when $-u = M^2$. Early data from SLAC are available [48]; more precise data are anticipated from JLab [49]. (Ref. [48] used the Meister-Yennie [9] soft corrections rather than those of Mo and Tsai. We have checked that for these kinematics the difference between them is smaller than 0.1%, which is negligible compared to the size of the error bars.)

E. Possibilities at lower $|u|$

In numerical calculations, we used a conservative requirement that the values of the Mandelstam variable $|u| > M^2$ in order to apply the partonic description. In a 'handbag' mechanism of wide-angle Compton scattering on a proton, such a requirement is needed to enforce high virtuality of the quark line between the two currents, making sure that short light-cone distances dominate. However, our case of electron–quark scattering via two-photon exchange involves 4-dimensional loop integration, and small values of $|u|$ do not necessarily mean that the struck quark has small virtuality. Analyzing the two-photon-exchange loop integral in terms of Sudakov variables one may show that for the backward $(u \to 0)$ electron–quark scattering, high virtuality of the quark dominates the loop integral, thereby justifying extension of our approach to the region of small u, as long as s and $-t$ remain large. Such an analysis may be found in the literature for the backward-angle electron-muon scattering in QED [50], and we found our formalism consistent with these early calculations.
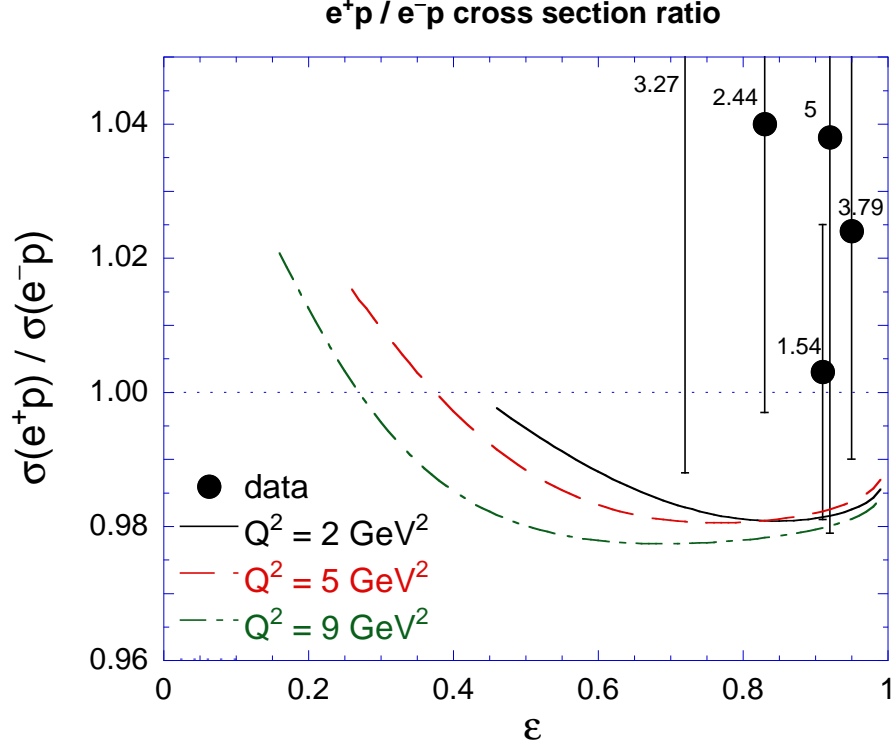
FIG. 8: Ratio of e^+/e^- elastic cross sections on the proton. The GPD calculations for the 2γ exchange correction are for three fixed Q^2 values of 2, 5, and 9 GeV^2, for the kinematical range where $-u$ is above M^2. Also shown are all known data, from [48], with Q^2 above 1.5 GeV^2 (the missing central value is at 1.111). The numbers near the data give Q^2 for that point in GeV^2.

F.   Rosenbluth determinations of G_E/G_M including 2-photon corrections

Previous Rosenbluth determinations of G_E/G_M were made using data which had been radiatively corrected using the Mo-Tsai [8] or comparable [9] prescription. Given the work in this paper, we would now say that these corrections are just a part of the total radiative correction. One should also include the hard two-photon corrections.

We present here new Rosenbluth determinations of G_E^p/G_M^p using known data but in-cluding the two-photon corrections. We used cross section data from Andivahis et $al.$ [6], and made a χ^2 fit to the data at each of the five Q^2 selected using our full calculation and allowing both G_M^p and G_E^p/G_M^p to vary. We included the lowest ε points in the data by making a linear extrapolation of our calculations from higher ε. (For the record, and for the ε's in question and to the precision we need, the result is numerically the same as doing our GPD calculation at these ε's, even though $|u|$ is below M^2.)

Rosenbluth w/2-γ corrections vs. Polarization data

Legend:
○ Pol.: Jones et al.
● Pol.: Gayou et al.
- - - Pol.: Gayou et al. fit
▽ Rosenbluth, Mo-Tsai corr. only
■ Rosenbluth, incl. 2γ corr. w/gauss. GPD

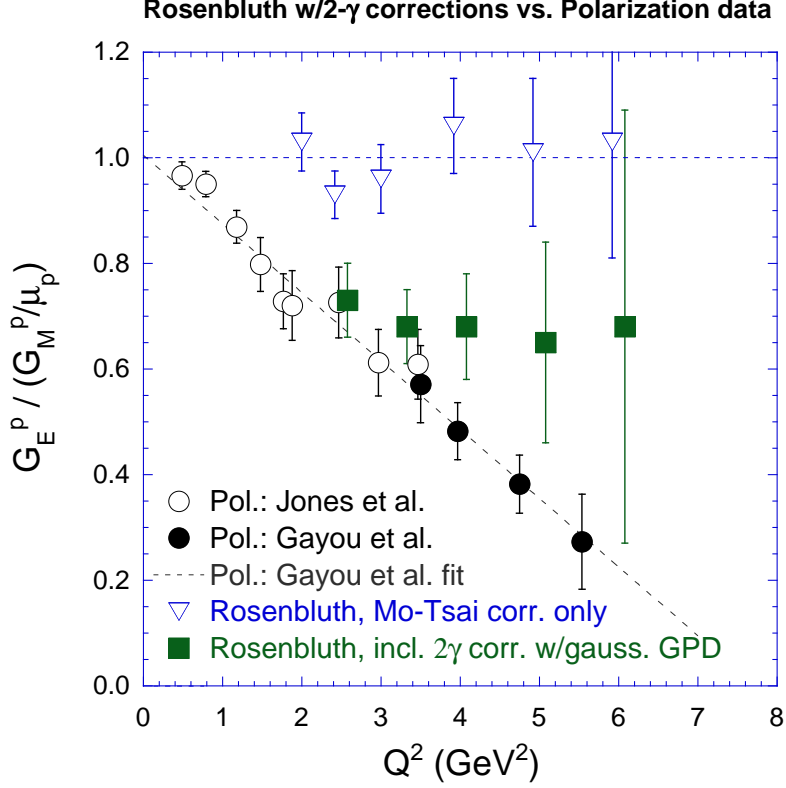Axes: $G_E^p / (G_M^p/\mu_p)$ vs. Q^2 (GeV^2)

FIG. 9: Rosenbluth determinations of G_E/G_M including the 2-photon corrections. The polarization data is from Jones *et al.* [1] and Gayou *et al.* [2], and the Rosenbluth determinations without the two-photon corrections are from [51]. The Rosenbluth G_E/G_M are based on data from Andivahis *et al.* [6]. Some of our points for the Rosenbluth results are slightly offset horizontally for clarity.

The results are shown in Fig. 9. The figure also shows the results of the polarization transfer measurements, and Rosenbluth results taken from [51], which do not include the hard two-photon corrections. The polarization results also have radiative corrections, but the size of them is, as one has learned from Fig. 6, smaller than the dots of the data points. The solid squares in Fig. 9 show the G_E/G_M ratios we have extracted with Ref. [6] data and the two-photon corrections with the gaussian GPD. The results with the modified Regge GPD are omitted to reduce clutter on the graph; they are about the same as for the gaussian for Q^2 of 2–3 GeV^2, and a bit larger at the higher Q^2.

For Q^2 in the 2–3 GeV^2 range, the G_E/G_M extracted using the Rosenbluth method including the two-photon corrections agree well with the polarization transfer results. At higher Q^2, there is at least partial reconciliation between the two methods.

One may comment on the growth of the error bars at higher Q^2. The calculation with

the two-photon contributions includes a lowest order term quadratic in G_E^p and a correction linear in G_E^p with opposite sign. The partial cancellation explains the reduced sensitivity to changes in G_E^p.

VI. CONCLUSIONS

We have studied the effects of two-photon physics for lepton-nucleon elastic scattering. Our main result is a calculation of the two-photon exchange contributions including contributions coming when intermediate particles which are far off shell. The main impediment to performing this calculation is the lack of knowledge of nucleon structure. Here we have used a partonic "handbag" model to express the contributions when both photons are hard in terms of the generalized parton distributions (GPD's) of the nucleon. The GPD's also enter calculations of deeply virtual Compton scattering, wide angle Compton scattering, and exclusive meson photoproduction, which are consistent with models for the GPD's. The calculations which we have presented are valid when s, $-u$, and Q^2 are large, although we have argued in subsection V E and Ref. [50], that the requirement on $-u$ is not compulsory for eN elastic scattering). We have presented our results requiring that the magnitude of each of the invariants is above M^2.

We have found that in Rosenbluth plots of the differential cross section vs. ε, that the two-photon exchange corrections gives an additional slope which is sufficient to reconcile qualitatively the difference between the Rosenbluth and polarization data. The change in the effective slope in the Rosenbluth plots comes only from corrections where both photons are hard. The reconciliation thus implies only a minor change in the G_E/G_M ratio as obtained from the polarization data, since those data receive smaller two-photon corrections to G_E/G_M.

Two-photon exchange has additional consequences which could be experimentally observed. For polarizations P_s and P_l, there are two-photon corrections which are small but measurable. For the normal direction, the polarization or analyzing power is zero in the one-photon exchange limit, but the presence of the two-photon exchange amplitude leads to a nonzero effect of $\mathcal{O}(1\%)$. We also predict a $\mathcal{O}(\text{few}\%)$ positron-proton/electron-proton asymmetry. The predicted Rosenbluth plot is no longer precisely linear; it acquires a measurable curvature, particularly at high ε.

Thus, in summary, we have shown that the hard two-photon exchange mechanism substantially reconciles the Rosenbluth and polarization transfer measurements of the proton electromagnetic elastic form factors. We have also emphasized that there are important experimentally testable consequences of the two-photon amplitude.

Acknowledgments

APPENDIX A: CROSS SECTION AND POLARIZATION RESULTS IN THE AXIAL-VECTOR REPRESENTATION

This appendix records the cross section and polarization results using the expansion of the scattering amplitude in the axial-vector representation given by Eq. (10),

$$
T_{h, \lambda'_N \lambda_N} = \frac{e^2}{Q^2} \left\{ \bar{u}(k', h) \gamma_\mu u(k, h) \times \bar{u}(p', \lambda'_N) \left[\gamma^\mu G'_M - \frac{P^\mu}{M} F'_2 \right] u(p, \lambda_N) \right.
$$
$$
\left. + \ \bar{u}(k', h) \gamma_\mu \gamma_5 u(k, h) \times \bar{u}(p, \lambda'_N) \, \gamma^\mu \gamma^5 G'_A \, u(p, \lambda_N) \right\} . \tag{A1}
$$

1. Form factors and observables

The scalar invariants or form factors are in general complex and functions of two variables. We also define

$$
G'_E \equiv G'_M - (1 + \tau) F'_2 . \tag{A2}
$$

The relations between the present scalar invariants and the ones used in most of the text follow from Eq. (11) and are

$$
G'_M = \tilde{G}_M + \frac{s - u}{4M^2} \tilde{F}_3
$$
$$
F'_2 = \tilde{F}_2
$$

$$G'_A = -\tau \tilde{F}_3$$

$$G'_E = \tilde{G}_E + \frac{s-u}{4M^2}\tilde{F}_3 \ . \tag{A3}$$

The invariants may be separated into parts coming from one-photon exchange and parts from two- or more-photon exchange,

$$G'_M = G_M + \delta G'_M \ ,$$

$$G'_E = G_E + \delta G'_E \ ,$$

$$G'_A = \delta G'_A \ , \tag{A4}$$

where $G_M(Q^2)$ and $G_E(Q^2)$ are the usual magnetic and electric form factors, defined from matrix elements of the electromagnetic current and real for spacelike Q^2. The quantities $\delta G'_M$, $\delta G'_E$, and G'_A are $\mathcal{O}(e^2)$ relative to G_M or G_E.

The reduced cross section in Eq. (14) is

$$\sigma_R = |G'_M|^2 + \frac{\varepsilon}{\tau}|G'_E|^2 + 2\sqrt{\frac{(1+\tau)(1-\varepsilon^2)}{\tau}}\, G_M\, \mathcal{R}\,(G'_A) + \mathcal{O}(e^4) \ . \tag{A5}$$

The polarizations of the outgoing nucleons or analyzing powers of the target nucleons are

$$P_n = A_n = \sqrt{\frac{2\,\varepsilon\,(1+\varepsilon)}{\tau}}\,\frac{1}{\sigma_R}\left\{\mathcal{I}(G'^*_E G'_M) + \sqrt{\frac{1+\tau}{\tau}\cdot\frac{1-\varepsilon}{1+\varepsilon}}\,G_E\,\mathcal{I}(G'_A) + \mathcal{O}(e^4)\right\} \ ,$$

$$P_s = A_s = -P_e\sqrt{\frac{2\varepsilon(1-\varepsilon)}{\tau}}\,\frac{1}{\sigma_R}\left\{\mathcal{R}\,(G'^*_E G'_M) + \sqrt{\frac{1+\tau}{\tau}\cdot\frac{1+\varepsilon}{1-\varepsilon}}\,G_E\,\mathcal{R}\,(G'_A) + \mathcal{O}(e^4)\right\} \ ,$$

$$P_l = -A_l = P_e\,\frac{1}{\sigma_R}\left\{\sqrt{1-\varepsilon^2}\,|G'_M|^2 + 2\sqrt{\frac{1+\tau}{\tau}}\,G_M\,\mathcal{R}(G'_A) + \mathcal{O}(e^4)\right\} \ . \tag{A6}$$

The only single spin asymmetry is P_n or A_n. Further, P_n or A_n is zero if there be only one-photon exchange, so observation of a non-zero value is definitive evidence for multiple-photon exchange. Polarizations P_s or P_l are double polarizations. The expressions for them are proportional to the electron longitudinal polarization P_e (with, e.g., $P_e = 1$ if $h = +1/2$).

2. Electron-quark elastic scattering amplitudes

The two-photon part of electron-quark elastic scattering is given by

$$H_{h,\lambda} = \frac{(e\,e_q)^2}{Q^2}\Big\{g_M\,\bar{u}(k',h)\gamma_\mu u(k,h)\,\cdot\,\bar{u}(p'_q,\lambda)\gamma^\mu u(p_q,\lambda)$$

$$+ g_A^{(2\gamma)} \; \bar{u}(k',h)\gamma_\mu\gamma_5 u(k,h) \cdot \bar{u}(p_q',\lambda)\gamma^\mu\gamma^5 u(p_q,\lambda)\Big\}$$

$$= \frac{(e\,e_q)^2}{Q^2}\Big\{\Big(\hat{s}-\hat{u}-(2h)(2\lambda)t\Big)g_M + \Big((2h)(2\lambda)(\hat{s}-\hat{u})-t\Big)g_A^{(2\gamma)}\Big\} , \qquad (A7)$$

when the electrons and quarks are both massless. The theorem of Eq. (11) relates

$$g_M = \tilde{f}_1 + \frac{\hat{s}-\hat{u}}{4}\tilde{f}_3 ,$$

$$g_A^{(2\gamma)} = \frac{t}{4}\tilde{f}_3 . \qquad (A8)$$

We split the two-photon part of g_M into a hard and soft part, $g_M^{(2\gamma)} = g_M^{soft} + g_M^{hard}$, using the prescription of Grammer and Yennie [31], and have

$$\mathcal{R}\left(g_M^{soft}\right) = \frac{\alpha}{\pi}\left\{\ln\left(\frac{\lambda^2}{\sqrt{-\hat{s}\hat{u}}}\right)\ln\left(\frac{\hat{s}}{-\hat{u}}\right) + \frac{\pi^2}{2}\right\} ,$$

$$\mathcal{I}\left(g_M^{soft}\right) = \alpha\ln\left(\frac{\hat{s}}{\lambda^2}\right) ,$$

$$\mathcal{R}\left(g_M^{hard}\right) = \frac{\alpha}{4\pi}\left\{\frac{-t}{\hat{u}}\ln\left(\frac{\hat{s}}{-t}\right) + \frac{t}{\hat{s}}\ln\left(\frac{\hat{u}}{t}\right)\right.$$
$$\left. + \frac{\hat{s}^2+3\hat{u}^2}{2\hat{u}^2}\ln^2\left(\frac{\hat{s}}{-t}\right) - \frac{3\hat{s}^2+\hat{u}^2}{2\hat{s}^2}\left(\ln^2\left(\frac{\hat{u}}{t}\right)+\pi^2\right)\right\} ,$$

$$\mathcal{I}\left(g_M^{hard}\right) = -\alpha\left\{\frac{\hat{s}^2+3\hat{u}^2}{4\hat{u}^2}\ln\left(\frac{\hat{s}}{-t}\right) - \frac{t}{4\hat{u}}\right\} ,$$

$$\mathcal{R}\left(g_M^{(2\gamma)}\right) = \frac{\alpha}{4\pi}\frac{t}{\hat{s}\,\hat{u}}\left\{\hat{s}\ln\left(\frac{\hat{s}}{-t}\right) + \hat{u}\ln\left(\frac{\hat{u}}{t}\right) + \frac{\hat{s}-\hat{u}}{2}\left[\frac{\hat{s}}{\hat{u}}\ln^2\left(\frac{\hat{s}}{-t}\right) - \frac{\hat{u}}{\hat{s}}\ln^2\left(\frac{\hat{u}}{t}\right) - \frac{\hat{u}}{\hat{s}}\pi^2\right]\right\} ,$$

$$\mathcal{I}\left(g_M^{(2\gamma)}\right) = -\alpha\frac{t}{4\hat{u}}\left\{\frac{\hat{s}-\hat{u}}{\hat{u}}\ln\left(\frac{\hat{s}}{-t}\right) + 1\right\} . \qquad (A9)$$

3. Embedding

The nucleon form factors are given in terms of the quark-level amplitudes and generalized parton distributions by

$$\delta G_M'^{(hard)} = \frac{1+\varepsilon}{2\varepsilon}A - \frac{1-\varepsilon}{2\varepsilon}C ,$$

$$\delta G_E'^{(hard)} = \sqrt{\frac{1+\varepsilon}{2\varepsilon}}B ,$$

$$\delta G_A'^{(hard)} = \frac{t}{s-u}\frac{1+\varepsilon}{2\varepsilon}(A-C) . \qquad (A10)$$

Quantities A, B, and C are the same as in the text, but now written as

$$A = \int_{-1}^{1}\frac{dx}{x}\frac{(\hat{s}-\hat{u})g_M^{hard}-tg_A^{(2\gamma)}}{s-u}\sum_q e_q^2\,(H^q+E^q),$$

31

$$B = \int_{-1}^{1} \frac{dx}{x} \frac{(\hat{s} - \hat{u})g_M^{hard} - tg_A^{(2\gamma)}}{s - u} \sum_q e_q^2 \left(H^q - \tau E^q \right),$$

$$C = \int_{-1}^{1} \frac{dx}{x} \frac{(\hat{s} - \hat{u})g_A^{(2\gamma)} - tg_M^{hard}}{-t} \text{sgm}(x) \sum_q e_q^2 \tilde{H}^q, \qquad \text{(A11)}$$

and it is understood in Eq. (A10) that the partonic amplitude g_M has its soft part removed.

APPENDIX B: QUARK MASS SENSITIVITY

1. Kinematics, and imaginary parts of the hard amplitudes

We have until now set the quark mass to zero.

To investigate how severe this approximation is, we will examine the effect of restoring the quark mass for the analyzing power calculations, though still keeping only the quark chirality conserving amplitudes. There are three modifications. The expressions for $\hat{s}$ and $\hat{u}$ become

$$\hat{s} = \frac{(x + \eta)^2}{4 \, x \, \eta} Q^2 + \frac{x + \eta}{x} m_q^2, \qquad \hat{u} = -\frac{(x - \eta)^2}{4 \, x \, \eta} Q^2 + \frac{x - \eta}{x} m_q^2, \qquad \text{(B1)}$$

where m_q is the effective quark mass. The general electron-quark scattering amplitude, Eq. (22), should have another term with a scalar function that we may call $\tilde{f}_2$ in analogy with the expansion of the electron-nucleon amplitude given in Eq. (12). However, this term flips quark helicities, and presently the formalism for embedding quark amplitudes into the nucleon using GPD's involves only the non-chirality flip GPD's. There is neither theoretical development nor experimental information regarding chirality flip GPD's, and so we shall ignore $\tilde{f}_2$ as well as helicity flip parts of other amplitudes. Including the quark mass leads to a modification of the hard scattering amplitudes so that

$$\frac{1}{2} \left[H_{h,+\frac{1}{2}}^{hard} + H_{h,-\frac{1}{2}}^{hard} \right] \overset{(m_q=0)}{=} \frac{e^2}{Q^2} \left\{ [\hat{s} - \hat{u}] \tilde{f}_1^{hard} - \hat{s}\hat{u}\tilde{f}_3 \right\}$$

$$\overset{\Rightarrow}{=} \frac{e^2}{Q^2} \left\{ \left[\hat{s} - \hat{u} - \frac{2m_q^2}{\hat{s} - m_q^2} Q^2 \right] \tilde{f}_1^{hard} + \left[m_q^4 - \hat{s}\hat{u} \right] \tilde{f}_3 \right\}, \quad \text{(B2)}$$

within the quantities A and B (C is not needed for the analyzing power), and

$$\mathcal{I}\left(\tilde{f}_1^{hard} \right) = -\frac{e^2}{4\pi} \left\{ \frac{\frac{1}{2}\hat{s}Q^2}{\hat{s}Q^2 - \left(\hat{s} - m_q^2\right)^2} \ln \left[\frac{\left(\hat{s} - m_q^2\right)^2}{\hat{s}Q^2} \right] + \frac{\hat{s} + m_q^2}{2\hat{s}} \right\},$$
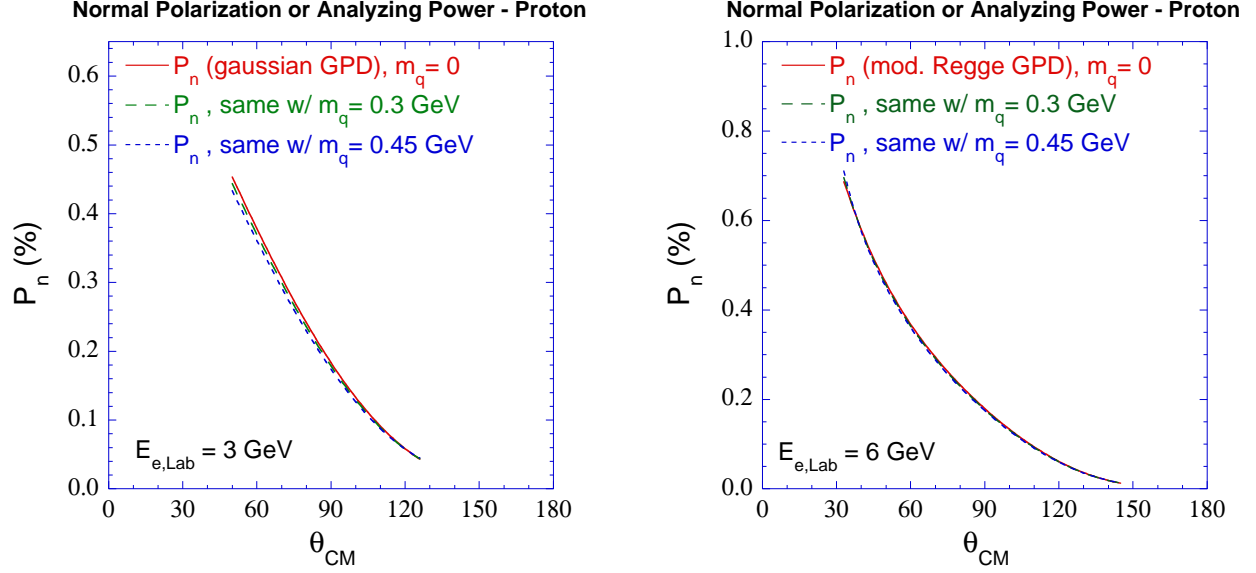
FIG. 10: Quark mass correction plots for the analyzing power or normal polarization, for fixed electron incoming lab energies of 3 and 6 GeV.

$$\mathcal{I}\left(\tilde{f}_3\right) = -\frac{e^2}{4\pi} \frac{\hat{s} - m_q^2}{\hat{s}Q^2 - \left(\hat{s} - m_q^2\right)^2}$$
$$\times \left\{ \frac{(\hat{s} - \hat{u})(\hat{s} - m_q^2)}{\hat{s}Q^2 - \left(\hat{s} - m_q^2\right)^2} \ln\left[\frac{\left(\hat{s} - m_q^2\right)^2}{\hat{s}Q^2}\right] + \frac{\hat{s} + m_q^2}{\hat{s}} \right\} . \tag{B3}$$

The results for the analyzing power A_n when including quark masses in the quark helicity conserving amplitudes are shown in Fig. 10 for quark masses 300 MeV and 450 MeV. The effects are clearly not large.

2.   Real parts of hard two-photon exchange amplitudes with finite quark mass

When the quark mass is not zero, we have

$$\mathcal{R}\left(\tilde{f}_1^{hard}\right) = \frac{e^2}{4\pi^2} \cdot \left\{ \left[\ln\left(\frac{\sqrt{(\hat{s} - m_q^2)|\hat{u} - m_q^2|}}{Q^2}\right) + \frac{1}{2}\right] \cdot \ln\left|\frac{\hat{s} - m_q^2}{\hat{u} - m_q^2}\right| \right.$$
$$+ \frac{m_q^2}{2}\left[\frac{1}{\hat{s}}\ln\left(\frac{\hat{s} - m_q^2}{m_q^2}\right) - \frac{1}{\hat{u}}\ln\left|\frac{\hat{u} - m_q^2}{m_q^2}\right|\right]$$
$$+ \frac{1}{2}\frac{Q^2(\hat{s} - \hat{u})}{(m_q^4 - \hat{s}\hat{u})}\left[\frac{\pi^2}{2} + \frac{1}{4}\ln^2\left(\frac{m_q^2}{Q^2}\right)\right] - \frac{1}{2}\ln^2\left(\frac{\hat{s} - m_q^2}{Q^2}\right) + \frac{1}{2}\ln^2\left|\frac{\hat{u} - m_q^2}{Q^2}\right|$$

33

$$+\frac{1}{2}\frac{(\hat{s}-\hat{u})(\hat{s}+\hat{u})}{(m_q^4-\hat{s}\hat{u})}\frac{1}{\chi}$$

$$\times\left[L\left(\frac{2}{1+\chi}\right)-\frac{\pi^2}{2}+\frac{1}{2}\ln\left(\frac{m_q^2}{Q^2}\right)\ln\left(\frac{1+\chi}{-1+\chi}\right)+\frac{1}{4}\ln^2\left(\frac{1+\chi}{-1+\chi}\right)\right]$$

$$-\frac{1}{2}\frac{Q^2\,\hat{s}}{(m_q^4-\hat{s}\hat{u})}\left[L\left(\frac{\hat{s}-m_q^2}{\hat{s}}\right)+\frac{1}{2}\ln^2\left(\frac{\hat{s}-m_q^2}{\hat{s}}\right)+\frac{1}{2}\ln^2\left(\frac{\hat{s}-m_q^2}{Q^2}\right)\right]$$

$$+\frac{1}{2}\frac{Q^2\,\hat{u}}{(m_q^4-\hat{s}\hat{u})}\left[-L\left(\frac{\hat{u}}{\hat{u}-m_q^2}\right)+\frac{5\pi^2}{6}+\frac{1}{2}\ln^2\left|\frac{\hat{u}-m_q^2}{Q^2}\right|\right]\Bigg\},\qquad(\mathrm{B}4)$$

and

$$\mathcal{R}\left(\tilde{f}_3\right)=-\frac{e^2}{4\pi^2}\frac{1}{(m_q^4-\hat{s}\hat{u})}\cdot\left\{\frac{\hat{s}^2-m_q^4}{\hat{s}}\ln\left(\frac{\hat{s}-m_q^2}{Q^2}\right)+\frac{\hat{u}^2-m_q^4}{\hat{u}}\ln\left|\frac{\hat{u}-m_q^2}{Q^2}\right|\right.$$

$$+\frac{(\hat{s}-\hat{u})^2Q^2}{(m_q^4-\hat{s}\hat{u})}\left[\frac{\pi^2}{3}+\frac{1}{4}\ln^2\left(\frac{m_q^2}{Q^2}\right)\right]+m_q^2\left(-2+\frac{m_q^2(\hat{s}+\hat{u})}{\hat{s}\hat{u}}\right)\ln\left(\frac{m_q^2}{Q^2}\right)$$

$$+\frac{(\hat{s}-\hat{u})^2(\hat{s}+\hat{u})+4m_q^2(m_q^4-\hat{s}\hat{u})}{(m_q^4-\hat{s}\hat{u})}\frac{1}{\chi}$$

$$\times\left[L\left(\frac{2}{1+\chi}\right)-\frac{\pi^2}{2}+\frac{1}{2}\ln\left(\frac{m_q^2}{Q^2}\right)\ln\left(\frac{1+\chi}{-1+\chi}\right)+\frac{1}{4}\ln^2\left(\frac{1+\chi}{-1+\chi}\right)\right]$$

$$+\frac{(\hat{s}-\hat{u})(\hat{s}-m_q^2)^2}{(m_q^4-\hat{s}\hat{u})}\left[-L\left(\frac{\hat{s}-m_q^2}{\hat{s}}\right)+\frac{\pi^2}{6}-\frac{1}{2}\ln^2\left(\frac{\hat{s}-m_q^2}{\hat{s}}\right)-\frac{1}{2}\ln^2\left(\frac{\hat{s}-m_q^2}{Q^2}\right)\right]$$

$$+\frac{(\hat{s}-\hat{u})(\hat{u}-m_q^2)^2}{(m_q^4-\hat{s}\hat{u})}\left[-L\left(\frac{\hat{u}}{\hat{u}-m_q^2}\right)+\frac{2\pi^2}{3}+\frac{1}{2}\ln^2\left|\frac{\hat{u}-m_q^2}{Q^2}\right|\right]\Bigg\},\qquad(\mathrm{B}5)$$

where $\hat{s}$ and $\hat{u}$ were given in Eq. (B1), and

$$\chi\equiv\sqrt{1+4m_q^2/Q^2}\,.\qquad(\mathrm{B}6)$$

The effect of the quark mass corrections upon the reduced cross section is shown in Fig. 11 for $Q^2=4$ GeV^2. One sees from Fig. 11 that the quark mass effects mainly influence our result at small values of ε, where $|u|$ becomes small. They show the theoretical error on our calculation in this region. A full calculation also requires quantifying the effect of the cat's ears diagrams. A study of such corrections is clearly worthwhile for a future work, both for two-photon exchange amplitudes and for wide-angle Compton scattering.

---

[1] M. K. Jones *et al.* [Jefferson Lab Hall A Collaboration], Phys. Rev. Lett. **84**, 1398 (2000) [arXiv:nucl-ex/9910005].
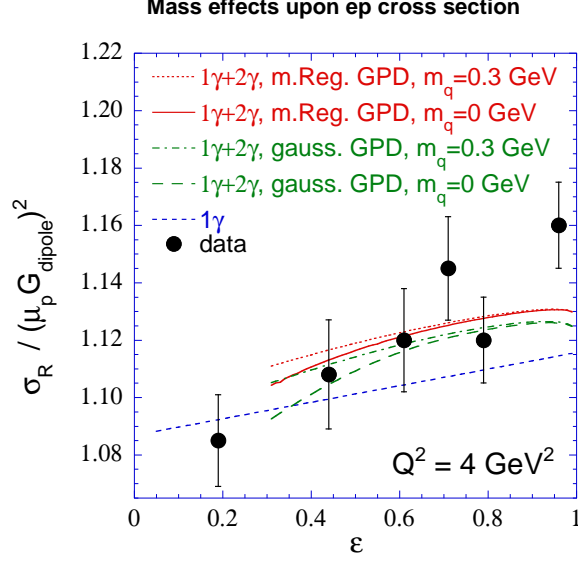
Mass effects upon ep cross section

FIG. 11: Quark mass correction plot for the reduced cross section. The curves are as labeled. In this plot, all curves have G_M set to 0.99 times the Brash *et al.* value [43]. The data is from [6].

[2] O. Gayou *et al.* [Jefferson Lab Hall A Collaboration], Phys. Rev. Lett. **88**, 092301 (2002) [arXiv:nucl-ex/0111010].

[3] A.I. Akhiezer, L.N. Rosentsweig, I.M. Shmushkevich, Sov. Phys. JETP **6**, 588 (1958); J. Scofield, Phys. Rev. **113**, 1599 (1959); *ibid.* **141**, 1352 (1966); N. Dombey, Rev. Mod. Phys. **41**, 236 (1969); A. I. Akhiezer and M. P. Rekalo, Sov. J. Part. Nucl. **4**, 277 (1974); R. G. Arnold, C. E. Carlson and F. Gross, Phys. Rev. C **23**, 363 (1981).

[4] M. E. Christy *et al.* [E94110 Collaboration], Phys. Rev. C **70**, 015206 (2004) [arXiv:nucl-ex/0401030].

[5] J. Arrington [JLab E01-001 Collaboration], arXiv:nucl-ex/0312017.

[6] L. Andivahis *et al.*, Phys. Rev. D **50**, 5491 (1994).

[7] P. A. M. Guichon and M. Vanderhaeghen, Phys. Rev. Lett. **91**, 142303 (2003) [arXiv:hep-ph/0306007].

[8] L. W. Mo and Y. S. Tsai, Rev. Mod. Phys. **41**, 205 (1969).

[9] N. Meister and D. R. Yennie, Phys. Rev. **130**, 1210 (1963).

[10] L. C. Maximon and J. A. Tjon, Phys. Rev. C **62**, 054320 (2000) [arXiv:nucl-th/0002058].

[11] A. Afanasev, I. Akushevich and N. Merenkov, Phys. Rev. D **64**, 113009 (2001) [arXiv:hep-ph/0102086].

[12] P. G. Blunden, W. Melnitchouk and J. A. Tjon, Phys. Rev. Lett. **91**, 142304 (2003) [arXiv:nucl-th/0306076].

[13] Y. C. Chen, A. Afanasev, S. J. Brodsky, C. E. Carlson and M. Vanderhaeghen, Phys. Rev. Lett. **93**, 122301 (2004) [arXiv:hep-ph/0403058].

[14] S. J. Brodsky and G. P. Lepage, Phys. Rev. D **24**, 1808 (1981).

[15] T. C. Brooks and L. J. Dixon, Phys. Rev. D **62**, 114021 (2000) [arXiv:hep-ph/0004143]; M. Vanderhaeghen, P. A. M. Guichon and J. Van de Wiele, Nucl. Phys. A **622**, 144C (1997); and private communication.

[16] S. J. Brodsky, F. E. Close and J. F. Gunion, Phys. Rev. D **8**, 3678 (1973).

[17] M. Damashek and F. J. Gilman, Phys. Rev. D **1**, 1319 (1970).

[18] S. J. Brodsky, F. E. Close and J. F. Gunion, Phys. Rev. D **5**, 1384 (1972).

[19] M. Diehl, T. Feldmann, R. Jakob and P. Kroll, Phys. Lett. B **460**, 204 (1999) [arXiv:hep-ph/9903268]; Eur. Phys. J. C **8**, 409 (1999) [arXiv:hep-ph/9811253].

[20] A. V. Radyushkin, Phys. Rev. D **58**, 114008 (1998) [arXiv:hep-ph/9803316].

[21] H. W. Huang, P. Kroll and T. Morii, Eur. Phys. J. C **23**, 301 (2002) [Erratum-ibid. C **31**, 279 (2003)] [arXiv:hep-ph/0110208].

[22] J. F. Gunion and R. Blankenbecler, Phys. Rev. D **3**, 2125 (1971). Dominance of double-scattering diagrams at large angles in the deuteron has been often noted; see, *e.g.,* C. E. Carlson, Phys. Rev. C **2**, 1224 (1970).

[23] I. A. Qattan *et al.*, arXiv:nucl-ex/0410010.

[24] Allan S. Krass, Phys. Rev. **125**, 2172 (1962).

[25] R. Ent, B. W. Filippone, N. C. R. Makins, R. G. Milner, T. G. O'Neill and D. A. Wasson, Phys. Rev. C **64**, 054610 (2001).

[26] M.L. Goldberger, Y. Nambu and R. Oehme, Ann. of Phys. **2**, 226 (1957).

[27] A. De Rujula, J. M. Kaplan and E. De Rafael, Nucl. Phys. B **35**, 365 (1971).

[28] A. Afanasev, I. Akushevich, and N. P. Merenkov, arXiv:hep-ph/0208260; M. Gorchtein, P. A. M. Guichon and M. Vanderhaeghen, Nucl. Phys. A **741**, 234 (2004) [arXiv:hep-ph/0404206]; L. Dixon and M. Schreiber, Phys. Rev. D **69**, 113001 (2004) [arXiv:hep-ph/0402221]; B. Pasquini and M. Vanderhaeghen, Phys. Rev. C **70**, 045206 (2004) [arXiv:hep-ph/0405303]; A. V. Afanasev and N. P. Merenkov, Phys. Lett. B **599**, 48 (2004) [arXiv:hep-ph/0407167] and Phys. Rev. D **70**, 073002 (2004) [arXiv:hep-ph/0406127].

[29] S. P. Wells *et al.* [SAMPLE collaboration], Phys. Rev. C **63**, 064001 (2001) [arXiv:nucl-ex/0002010]; F. E. Maas *et al.*, arXiv:nucl-ex/0410013.

[30] P. Van Nieuwenhuizen, Nucl. Phys. B **28**, 429 (1971).

[31] G. J. Grammer and D. R. Yennie, Phys. Rev. D **8**, 4332 (1973).

[32] V. V. Bytev, E. A. Kuraev and B. G. Shaikhatdenov, J. Exp. Theor. Phys. **96**, 193 (2003) [Zh. Eksp. Teor. Fiz. **123**, 224 (2003)]; J. Exp. Theor. Phys. **95**, 404 (2002) [Zh. Eksp. Teor. Fiz. **122**, 472 (2002)] [arXiv:hep-ph/0203127].

[33] I. B. Khriplovich, Yad. Fiz. **17** (1973) 576; R. W. Brown, K. O. Mikaelian, V. K. Cung and E. A. Paschos, Phys. Lett. B **43**, 403 (1973).

[34] A.O. Barut and C. Fronsdal, Phys. Rev. **120**, 1871 (1960).

[35] For a general discussion, see S. J. Brodsky and J. R. Primack, Annals Phys. **52**, 315 (1969).

[36] S. D. Drell and T. M. Yan, Phys. Rev. Lett. **24**, 181 (1970).

[37] S. J. Brodsky, F. E. Close and J. F. Gunion, Phys. Rev. D **5**, 1384 (1972).

[38] K. Goeke, M. V. Polyakov and M. Vanderhaeghen, Prog. Part. Nucl. Phys. **47**, 401 (2001) [arXiv:hep-ph/0106012].

[39] A. D. Martin, R. G. Roberts, W. J. Stirling and R. S. Thorne, Phys. Lett. B **531**, 216 (2002) [arXiv:hep-ph/0201127].

[40] E. Leader, A. V. Sidorov and D. B. Stamenov, Eur. Phys. J. C **23**, 479 (2002) [arXiv:hep-ph/0111267].

[41] F. Yuan, Phys. Rev. D **69**, 051501 (2004) [arXiv:hep-ph/0311288].

[42] M. Guidal, M. Polyakov, A. Radyushkin, and M. Vanderhaeghen, arXiv:hep-ph/0410251.

[43] E. J. Brash, A. Kozlov, S. Li and G. M. Huber, Phys. Rev. C **65**, 051001 (2002) [arXiv:hep-ex/0111038].

[44] G. Kubon *et al.*, Phys. Lett. B **524**, 26 (2002) [arXiv:nucl-ex/0107016].

[45] R. Madey *et al.* [E93-038 Collaboration], Phys. Rev. Lett. **91**, 122002 (2003) [arXiv:nucl-ex/0308007]; see also G. Warren *et al.* [Jefferson Lab E93-026 Collaboration], Phys. Rev. Lett. **92**, 042301 (2004) [arXiv:nucl-ex/0308021].

[46] JLab experiment E-05-015, spokespersons T. Averett, J.P. Chen, X. Jiang.

[47] JLab experiment E-04-019, spokespersons R. Gilman, L. Pentchev, C. Perdrisat, and R. Suleiman.

[48] J. Mar *et al.*, Phys. Rev. Lett. **21**, 482 (1968).

[49] Jefferson Lab experiment E-04-116; contact person, W. Brooks.

[50] V. G. Gorshkov, V. N. Gribov, L. N. Lipatov, and G. V. Frolov, Sov. J. Nucl. Phys. **6**, 95 (1968) [Yad. Fiz. **6**, 129 (1967)]; also in V. B. Berestetskii, E. M. Lifshitz, and L. P. Pitaevskii, Quantum Electrodynamics, Course of Theoretical Physics, Vol. 4, Second edition (Pergamon Press, Oxford and New York, 1982), pp. 616ff.

[51] J. Arrington, Phys. Rev. C **68**, 034325 (2003) [arXiv:nucl-ex/0305009].